Climate Change, Population Growth, and Population Pressure*

J. Vernon Henderson, Bo Yeon Jang, Adam Storeygard, and David N. Weil

January 2024

Abstract

We develop a novel method for assessing the effect of constraints imposed by spatially-fixed natural resources on aggregate economic output. We apply it to estimate and compare the projected effects of climate change and population growth over the course of the 21st century, by country and globally. We find that standard population growth projections imply larger reductions in income than even the most extreme widely-adopted climate change scenario (RCP8.5). Climate and population impacts are correlated across countries: climate change and population growth will have their most damaging effects in similar places. Relative to previous work on macro climate impacts, our approach has the advantages of being disciplined by a simple macro growth model that allows for adaptation and of assessing impacts via a large set of climate moments, not just annual average temperature and precipitation. Further, our estimated effects of climate are by construction independent of country-level factors such as institutions.

*Henderson: London School of Economics. Jang: Brown University. Storeygard: Tufts University. Weil: Brown University. We are grateful to Lint Barrage, Greg Casey, Maureen Cropper, Eric Galbraith, and Zeina Hasna for helpful advice; to Lucy Li, Frankie Fan, William Yang, and Raymond Yeo for research assistance; to David Anthoff, Brian Prest, and Lisa Rennels for access to data and code; and to seminar audiences at the Bank of Italy, University of Bologna, Université Catholique de Louvain, University of Chicago, University of Chile, University of Connecticut, ETH Zurich, IIASA, Korea University, Lahore School of Economics, University of Manchester, NYU Abu Dhabi, Osaka University, Oxford University, RIDGE forum on Sustainable Growth, Schumpeter Seminar (Humboldt University), Sungkyunkwan University, University of Tokyo, and the World Bank for useful feedback. Research was supported by the Population Studies and Training Center at Brown University through the generosity of the Eunice Kennedy Shriver National Institute of Child Health and Human Development (P2C HD041020 and T32 HD007338).

1 Introduction

Climate change over the coming decades will affect the ability of land to support the lives and livelihoods of much of the world's population. This is most obvious in the case of agricultural productivity, which will be strongly affected by changes in rainfall and temperature. In addition, climate change may lower the quality of life in given regions or require the expenditure of additional resources to maintain a specific quality of life. Beyond reductions in the standard of living, these changes are expected to impact the frequency of conflict as well as flows of population, including migrants and refugees.

Many, though not all, of the economic and social effects of climate change can be understood through the lens of population pressure on fixed local factors of production. The distribution of population in space reflects heterogeneity in these factors: some places are more productive and easier to live in than others, and the places where production and life are easier tend to be where people concentrate. Climate change will alter some of these characteristics, making some locations more attractive and others less so. A decline in the services provided by local fixed factors, what we call the "quality" of a location, means that the standard of living will decline or that some of the people in a location will be induced to move elsewhere.

Our paper makes two contributions. The first is a new methodology for projecting the economic impact of forecast changes in climate at the grid cell, country, and world levels. Our methodology takes advantage of spatial variation in characteristics that will be altered by climate change in order to estimate weights on different climate components. Notably, we use a large set of climate indicators from global climate models, going beyond the simple annual averages of temperature and precipitation used in most existing research to include intra-annual variation in both temperature and precipitation, frequency of temperature extremes, and suitability for many specific crops, among other measures. We econometrically assign weights to these multiple dimensions based on their effects on the within-country spatial distribution of population observed today. We pair the results of this econometric exercise with a macroeconomic growth model, which allows us to examine, among other things, the effects of within-country labor mobility. The general tenor of the projections that we produce is in line with a good deal of previous work, specifically in finding that negative economic effects of climate change will be most severe in poorer and

hotter countries, while several colder regions may benefit. But there are significant quantitative differences between our findings and previous research.

The second contribution is to bring together the analysis of climate change and population growth into a single framework, through the lens of population pressure on local resources. Population pressure rises when location quality declines or when population size rises. Our framework allows us both to study the combined impact of these two forces, and to compare their relative magnitudes. Many countries, especially lower income ones that are expected to suffer degradation in location quality due to climate change are also expected to see large increases in the population that will be reliant on that land. Further, the impacts of population growth on reducing 2100 GDP per capita are typically greater than those due to climate change. Finally, looking across the range of projections, uncertainty regarding the effect of population on economic outcomes appears to be bigger than uncertainty regarding the effect of climate change.

The rest of this paper is structured as follows. Section 2 briefly reviews the literatures on the effects of both climate change and population growth on economic outcomes. Section 3 discusses our methodology for estimating location quality and how it will be affected by projected climate change. In Section 4, we present our estimates of climate effects on location quality at the world, continent, and country levels. Section 5 lays out the economic model that is used to map from changes in climate and population into changes in GDP per capita, and also discusses the role of within-country labor mobility as means of adapting to climate change. Then Section 6 presents projected country-level impacts from climate change alone as well as from climate and population combined. This section also discusses variability across climate and population projections. Section 7 aggregates projected damages from climate change to the world level to facilitate comparison with other estimates, and also examines the effect of projected climate change on cross-country income inequality. Section 8 concludes.

2 Previous Literature

2.1 Climate change

The economic effects of climate change are frequently summarized in the form of a damage function that relates the loss in GDP relative to what it would have been in

the absence of climate change to the extent of climate change, as measured by the increase in atmospheric carbon dioxide or the global rise in mean surface temperature. Broadly, there are two approaches to estimating the damage function (Hsiang, 2016; Massetti and Mendelsohn, 2018). The first looks cross-sectionally to compare economic outcomes in locations with different climates in the present, and then applies the estimated effects of climate differences to projected changes in climate in the future. This approach has the advantage of assessing climate effects after accounting for any adaptations (such as infrastructure and choice of crops) embodied in the current cross section. However, it faces the challenge that cross sectional variation in climate may be correlated with unobserved variables, such as institutions, that impact the economy. For this reason, research in this line tends to use within-country variation as a source of identification.

In a work related to ours, Nordhaus (2006) applies this approach, regressing total GDP in grid cells covering the whole world on annual mean temperature and precipitation, geographical controls, and country fixed effects. His estimate is that in the scenario where global mean surface temperature rises by 3 degrees C, global output damage would be 3.0%. Our work differs from Nordhaus (2006) in a number of important dimensions. We assess the effects of climate change in parallel with (and in comparison to) the effects of population growth, and this assessment is carried out using a macroeconomic growth model, rather than being purely statistical. The use of a model also allows us to consider different scenarios regarding population migration in response to climate change. In terms of data, we use a broader set of climate attributes than simply average temperature and precipitation. Finally, instead of a log-linear specification, we estimate a Poisson model, which we show to be a significant methodological improvement.

The alternative approach to estimating the damage function looks at the relationship between changes in outcomes such as temperature and precipitation, on the one hand, and output or other economic or social outcomes, on the other. The advantage of this approach is that it differences out any fixed unobserved characteristics that may be correlated with climate. The greatest challenge it faces is dealing with adaptation. Hsiang (2016) and Lemoine (2021) discuss the assumptions required to estimate the effects in climate change through variation in weather.

Dell et al. (2012) examine the effects of current and lagged annual average temperature on income growth. They find a negative effect of temperature shocks on

income growth in poor but not rich countries. They caution that, because their results are for short run fluctuations, they are not necessarily applicable to analyzing the effects of climate change, although they do find similar results in a medium-run analysis that looks at 15 year differences. Burke et al. (2015a) regress annual GDP growth (rather than level) on average annual temperature and its square in a panel of countries over the period 1960–2010. They find dramatic effects, with world GDP in 2100 23% lower than in the absence of warming.[1] Cruz and Rossi-Hansberg (forthcoming) use a similar empirical strategy in estimating a damage function that serves as an input to their dynamic climate assessment model. In that model, the starting point is a set of location-specific productivity and amenity values, which are derived from solving and inverting a spatial growth model that includes trade, migration, and local innovation, using grid cell data on wages, population, land, and energy prices.[2]

A number of papers have compiled damage function estimates from several different sources and estimated an average worldwide damage function from them. For example, the DICE-2023 model (Barrage and Nordhaus, 2023) embeds a damage function relating lost GDP to the square of the deviation of global average surface temperature from its historical mean. The damage coefficient is derived from fitting a quadratic model to 56 existing estimates of damages under different climate change scenarios and then adding adjustments for potential climate tipping points as well as a judgmental adjustment term to reflect omitted non-monetized impacts (such as loss of biodiversity) and uncertainty. The estimates imply that a rise in mean temperature of 3 degrees C would reduce world GDP by roughly 3.1%, and a 6 degree rise would reduce global income by 12.5%.[3] According to Stocker et al. (2013), the rise in mean surface temperature by the period 2081–2100 is likely to fall into the range of 2.6–4.8 degrees under the RCP 8.5 emissions pathway where there is continuing high use of fossil fuels worldwide.

Much of the recent literature discussing climate change in a spatial framework depends on these damage functions to incorporate warming into models. Desmet and Rossi-Hansberg (2015) use a similar damage function to that of the DICE model.

[1] Casey et al. (2023) critique this approach. Similar recent analyses include Kahn et al. (2021), Tol (2021), and Newell et al. (2021).

[2] As an alternative to estimating economy-wide damage functions, a number of papers look at specific sectors or outcomes. These include Costinot et al. (2016), who examine the impact of climate change on agriculture, and Carleton et al. (2022), who examine mortality outcomes. Implicitly, a measure of overall damage from climate change could be derived by summing these channels.

[3] Other compilations of damage estimates include Tol (2012) and Piontek et al. (2021).

Krusell and Smith (2022) likewise calibrate their regional damage functions to match the global damage function estimate from DICE-2016.

In addition to the expected effects on GDP, research has also looked at impacts of climate change in many other dimensions, with two of the most notable being conflict and migration. Burke et al. (2015b) and Harari and Ferrara (2018) examine the effect of climate on civil conflict. McGuirk and Nunn (forthcoming) show that climate change has already driven increasing conflict between transhumant pastoralists and sedentary agriculturalists in Africa. Rigaud et al. (2018) project that as of 2050, 2.8% of the population in the group of developing countries that they study, or 143 million people, will have had to migrate internally. Similarly Burzyński et al. (2022) project that 62 million working age adults will have to move, most of them within their own countries, because of climate during the 21st century.[4] A 2021 U.S. government report predicted that over time an increasing fraction of this migration will be across national borders (White House, 2021).

2.2 Population Pressure

The literature studying the economic and social effects of climate change described above is mostly a product of the last several decades. By contrast, literature on the effects of natural resource congestion due to population growth is far older, going back at least to Malthus (1798). Authors such as Hardin (1968), and Ehrlich (1968) focused on the inability of existing natural resources to support ever-growing populations. More recent literature arguing that the resource congestion channel has an important impact on economic outcomes, particularly in poor countries, includes Young (2005), Acemoglu and Johnson (2007), and Kohler (2012). Das Gupta et al. (2011) point out that discussion of "sustainable development" at the country level is to a large extent simply a reformulation of the Malthusian concern with the ratio of population to resources. Paralleling the more recent literature on climate change and conflict, Acemoglu et al. (2020) show that higher growth in population resulted in increases in civil wars and other measures of social conflict. Similarly, pressure on natural resources due to population growth is a hypothesized driver of both internal and international migration.

Although research on this topic does not use the terminology of a damage function, there is no barrier to applying the same concept. For example, the IV estimates in

[4]See also Lustgarten (2020a,b,c).

Acemoglu and Johnson (2007) imply that a change in life expectancy that raised population by 1% would lower GDP per capita by 0.79%.[5] Similarly Ashraf et al. (2013), using a simulation model parameterized to match Nigeria, find that an increase in fertility that raised population by 16.6% would reduce income per capita by 10.6%.[6]

Existing literature does not address the relative magnitude of economic stress due to climate change, on the one hand, and population growth, on the other. To the extent that the two issues are discussed together, it is often in the context of how population affects carbon emissions, and through this channel climate (Casey and Galor, 2017).[7]

3 Projecting Climate Impacts on Location Quality

Our approach follows broadly in the mode of the cross section approach discussed above, most notably Nordhaus (2006). The key insight is that one can infer the characteristics that affect location quality, and the appropriate weights to apply to them, by looking at current settlement patterns. In order to assess the effects of changes in location quality due to climate change and the effects of population pressure on both resource congestion and growth, we gather information for two periods: roughly current day, encompassing data from 1980 to 2010, and the future, for which we use projections for 2071 to 2100. For convenience, we refer to the former as 2010 and the latter as 2100.

3.1 Empirical Model

We outline a simple model of population allocation within a country that leads directly to our econometric specification. Production in grid cell i of country c is given by

$$Y_{i,c} = (Q_{i,c}Z_{i,c})^{\phi} K_{i,c}^{\alpha} (e_c L_{i,c})^{1-\alpha-\phi} \tag{1}$$

where $Q_{i,c}$ is a measure of location quality, $Z_{i,c}$ is land area, e_c is a country-level measure of productivity due to non-land factors (institutions, technology, etc.), $K_{i,c}$ is physical capital, and $L_{i,c}$ is labor. Differences in human capital per worker could also be incorporated into e_c. Similarly, allowing for agglomeration economies would

[5] Tables 8 and 9, column 1.

[6] Values for the year 2060, comparing the UN low and medium fertility projections.

[7] Vörösmarty et al. (2000) discuss the interaction of climate change and population growth in the particular case of demand placed on local freshwater resources.

not affect the key results of the model for our purposes.[8] Although the regions that we use are all quarter-degree squares of latitude and longitude, they differ in their land areas both because lines of longitude converge away from the equator and because parts of some grid squares are covered with water.

Labor and capital are assumed to be perfectly mobile within countries to equalize their marginal products across grid cells. This implies that in equilibrium, within a country, grid cell density, $L_{i,c}/Z_{i,c}$, will be proportional to the location quality of the grid cell. Quality in turn is postulated to be a function of the vector of geographic characteristics, $x_{i,c}$, of the grid cell, $Q_{i,c} = exp(x_{i,c}\beta)$. Thus

$$L_{i,c}/Z_{i,c} = exp(x_{i,c}\beta)C_c, \tag{2}$$

where C_c is a country fixed effect that ensures that we are identifying quality exclusively from variation in population density that is within-country and therefore not driven by differences across countries in institutions, technology, culture, or historical development.

Estimated location quality for each grid cell is the fitted value from (2), excluding country fixed effects. That is, we define

$$\hat{Q}_{i,c} = \exp(x_{i,c}\hat{\beta})\Big[\frac{\sum Z_{i,c}}{\sum \exp(x_{j,c}\hat{\beta})Z_{j,c}}\Big]. \tag{3}$$

where $\hat{\beta}$ is the vector of estimated coefficients from equation (2). The term in brackets is a normalization such that the worldwide sum of quality-adjusted area $\hat{Q}_{i,c}Z_{i,c}$ is equal to the actual land area of the world.

While the discussion has focused on location productivity, it is straightforward to extend the model so that the vector of land characteristics affects not only productivity but also the amenity value of a location. The extension simply affects the interpretation of the coefficients and not the estimates of location quality.[9]

[8] If we think that agglomeration economies come from density as in the classic Ciccone and Hall (1996) paper or more modern papers such as Combes et al. (2017) and Henderson et al. (2021), then the right hand side of (1) should be multiplied by $(L_{i,c}/Z_{i,c})^{\eta}$. In this case, equation (4) is the same, except instead of estimating β, we estimate $\beta\phi/(\phi - \eta)$. Using a typical value of $\eta = 0.04$ from the literature (see Rosenthal and Strange, 2004; Combes and Gobillon, 2015) and 0.25 for ϕ as discussed below, $\phi/(\phi - \eta) = 1.19$. While this affects the interpretation of the estimated coefficients in (4), it does not affect the fitted values from this equation, our focus below.

[9] Let the amenity value of a grid square be $A_{i,c} = exp(x_{i,c}\gamma)$ and assume mobility within a country equalizes the product of the average product of labor and amenities. In this case, $E(\hat{\beta}) = \beta + \gamma$.

3.2 Data and Specification

For the dependent variable in (2), we use the European Union's Global Human Settlements population layer (GHS-POP). In Appendix B we discuss the comparison of results using this population dataset with those obtained using two others: the Gridded Population of the World version 4 and LandScan.

Geographic characteristics, $x_{i,c}$, include elevation, latitude, ruggedness, distance to the coast, and a set of four dummies indicating the presence of a coast, a navigable river, a major lake, and a natural harbor within 25 km of a cell centroid, all from Henderson et al. (2018). From the U.N. Food and Agricultural Organization's Global Agro Ecological Zones v4 dataset (FAO's GAEZ) we add a selection of 33 characteristics that provide information on the thermal regime, moisture regime, and growing period of each grid square as well as suitability indices of 11 major crops, all for the time period 1981–2010. Also included is the maximum potential caloric yield across these 11 crops, calculated using the methodology established by Galor and Özak (2016). To assess the effect of climate variability, we include a measure of year-to-year volatility of daily temperature. These data are collected for 237,023 quarter-degree grid squares in 164 countries. Appendix A discusses the data and methodology in greater detail.

Previous work (Nordhaus, 2006; Henderson et al., 2018) estimated the parameters in equation (2) by taking logs and including an additive error term. There are three key problems with this log-linear specification, however. First, 40% of grid squares in our data have zero reported population. While a strict application of the model suggests there should be no zeros, we believe the volume of zeros largely reflects measurement error (discussed in Appendix B) as well as restrictions on where people are permitted to live.[10] A common approach to this problem is to replace these zeros with a small non-zero value.[11] Unfortunately, parameter estimates can be sensitive to the value used for imputation, and are also sensitive to simply dropping zeros.

Second, as seen in Figures B1.A and B1.B, many grid cells in the world have

[10] According to the United Nations Environment Programme (2016), 14.7% of the world's land area is in "protected areas" such as national parks.

[11] For example, Henderson et al. (2018), which examined lights data, assigned to every reported zero observation the minimum non-zero value in the dataset. In Nordhaus (2006), where output per square kilometer is the dependent variable, 3,170 of 17,409 grid squares in the regression sample have zero values for the dependent variable. Nordhaus imputes values for 618 of these cells based on neighbors, and then assigns the remainder a value of one before taking logs.

extremely low population densities. For example, in the GHS data 75% have density less than 12 people per square kilometer, while 98.5% of the world's population lives in grid squares with density above this level. As discussed in Appendix B, data construction issues are likely to introduce a good deal of measurement error in sparsely populated regions, and even to the extent that density in these regions is correctly measured, its determinants are conceptually of less interest than the determinants of density in regions where most people live. The log-linear specification, however, places a lot of weight on regions with extremely low population densities.

Third, Santos Silva and Tenreyro (2006) show that OLS estimates of a log-linear version of (2) are inconsistent (and NLS inefficient) in the presence of heteroskedasticity, which is likely in our context. These issues are discussed more extensively in Appendix B.

For these reasons we estimate a Poisson model. The specific functional form is

$$E(L_{i,c}/Z_{i,c} \mid C_c, x_{i,c}) = exp(C_c + x_{i,c}\beta) \tag{4}$$

The Poisson specification is well-suited for outcome measures with many zeros and tiny values. As shown in Appendix Figure B2, predicted values of density from a Poisson specification are remarkably robust to using the two alternative population datasets noted above, while log-linear predicted values are not.

The stochastic component of our model is crucial for addressing the contingent nature of human settlement. There is a vast literature on multiple equilibria and accidents of history with agglomeration (e.g. Krugman, 1991; Arthur, 1989; Davis and Weinstein, 2002). More recent work has focused on dynamic development subject to stochastic processes that yield particular, unique equilibria as a way of encapsulating these accidents (Michaels et al., 2012; Desmet and Rappaport, 2017). For example, in a model similar to ours but with a more complex production process, Desmet and Rappaport envision regions as being subject to initial large productivity/resource shocks and then to a series of smaller accumulating independent draws over time. These accidents are important to understanding why, for example, the centre of Kolkata is not 50 kilometers further up or down the Hugli River or on a completely different river in historical Bengal. In that particular case, an initial arbitrary choice of a British East India Company employee, Job Charnock, and then a history of other choices and accumulations over 300 years, anchored that location

and induced high density. Our reduced form specification summarizes the cumulative impact of such a succession of shocks. Since we are assuming a Poisson specification overall, we effectively assume that these shocks are a series of Poisson draws.

The country fixed effects in (4) control for factors like technology and national population relative to national land area. Identification of the determinants of location quality comes solely from within-country variation. In other words, β is not estimated by comparing the land characteristics of more and less densely populated countries, but rather by comparing variation in land characteristics and population density within countries.

3.3 Projecting Climate Impacts

Climate change will alter many of the characteristics that determine our measure of location quality. A key innovation in the present paper is to substitute projections of future characteristics into equation (3), allowing us to calculate expected future location quality at the grid cell level:

$$\hat{Q}_{i,c,2100} = exp(x_{i,c,2100}\hat{\beta})\Big[\frac{\sum Z_{i,c}}{\sum exp(x_{j,c,2010}\hat{\beta})Z_{j,c}}\Big]. \tag{5}$$

In essence, to calculate grid-cell location quality for 2100, we apply the $\hat{\beta}$ coefficients from (4) estimated on 2010 data to future projections of the geographic characteristics. The term in brackets maintains the 2010 normalization from equation (3), so that global average Q in year 2100 is measured relative to 2010.

Projections of future climatic conditions are generated by global climate models. These are numerical representations of the earth's climate, in which future states of the world are derived from initial conditions using physical laws. As such, the outputs of these models are highly dependent on the assumed trajectory of carbon concentrations from current day to the date of the projection. To ensure that these outputs are comparable, the Intergovernmental Panel on Climate Change (IPCC) has established four scenarios of future greenhouse gas concentrations, called Representative Concentration Pathways (RCPs), as standard inputs for the various models. Each scenario is characterized by an increase in radiative forcing (in watts per square meter), relative to preindustrial conditions, in 2100. RCP 2.6 traces the best-case trajectory while RCP 8.5 depicts conditions from sustained aggressive fossil fuel use. GAEZ provides projections for all four scenarios from five different climate models used in the IPCC's

fifth assessment report. Our main results take the average of future grid cell quality in each of the climate models calculated using the coefficients from the 2010 regression, then aggregate these cell quality values within countries. In Appendix C, we compare our predictions for changes in location quality between 2010 and 2100 across the five climate models and the ensemble mean. They are highly correlated with each other and, then, obviously with the mean. The larger deviations occur in countries where location quality is expected to improve dramatically, rather than in countries where location quality will deteriorate. We focus on the latter group, which includes nearly all poor and middle-income countries.

Our measure of quality is based on a worldwide grid square regression. A potential concern is that the value of specific land characteristics in determining economic outcomes may be a function of the level of a country's development. For example, a reduction in rainfall could be devastating in a region reliant on rain-fed agriculture, but in a richer region that imports its food from elsewhere it would have only a marginal effect. We address this concern in Appendix D, where we estimate equation (4) using a sample of grid squares solely from countries with below-median income and then solely from countries with above median income. In Figure D1, we then compare the predicted changes in GDP per capita by country (using the methodology presented below) between each of these and our baseline. The results are highly correlated in both cases.

4 Projected Effects of Climate Change on Location Quality

This section begins by reporting the estimated effects of climate change on location quality at the grid square level and then aggregates up to look at world, region, and country impacts on average location quality. Impacts are heterogeneous across the world: Some countries will experience improvements, while many others, especially poorer ones, will see significant deterioration.

4.1 Grid Cell, Global, and Regional Results

We start at the grid square level. The first panel of Figure 1 shows our estimated values of log 2010 location quality. The second panel then shows projected changes in location quality between 2010 and 2100 under RCP 8.5. In general, the areas with improvements in location quality are mountainous and/or distant from the equator.

Location quality declines in almost all of Africa and Australia as well as large parts of South America and central, south, and southeast Asia. The northernmost parts of Europe are projected to benefit, along with most of Canada and Russia. There is a good deal of internal variation within larger countries. For example, within the United States, the Gulf coast suffers declines in location quality while in much of the mountain west it improves.

Figure 1: Log Location Quality

(a) Historical Log Location Quality

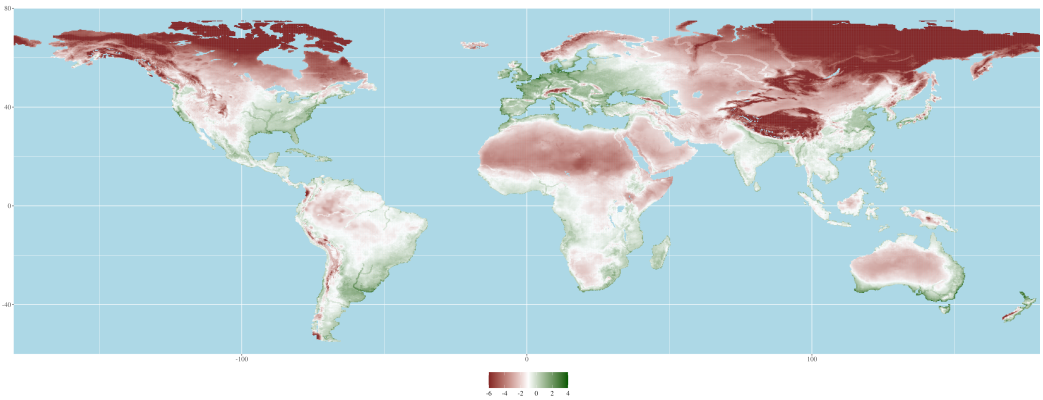

(b) Differences between Historical and 2071–2100 Log Location Quality under RCP 8.5

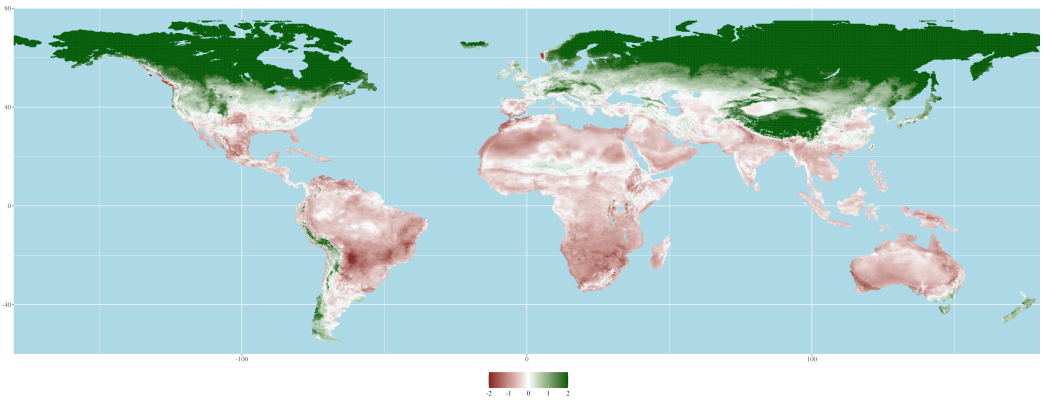

Notes: Data are censored at -6 and 4 and at -2 and 2 in the top and bottom panels, respectively, for visualization. Plate Carrée projection.

To examine heterogeneity in the distribution of projected changes in location quality, we plot in Figure 2 histograms for grid cells in countries whose 2010 GDPs were either above or below the median. In the top row, the vertical axis represents the percentage of the country group's total land area that falls into each bin; in the bottom, it represents the percentage of the country group's total 2010 population.

Among countries with below-median GDP per capita, 72% of the land area, hosting 83% of the current population, is expected to see a decrease in location quality. By contrast, among countries with above-median GDP per capita, only 47% of land area, hosting 52% of the population is expected to see such a decrease.

Figure 2: Histograms of Changes to Log Location Quality

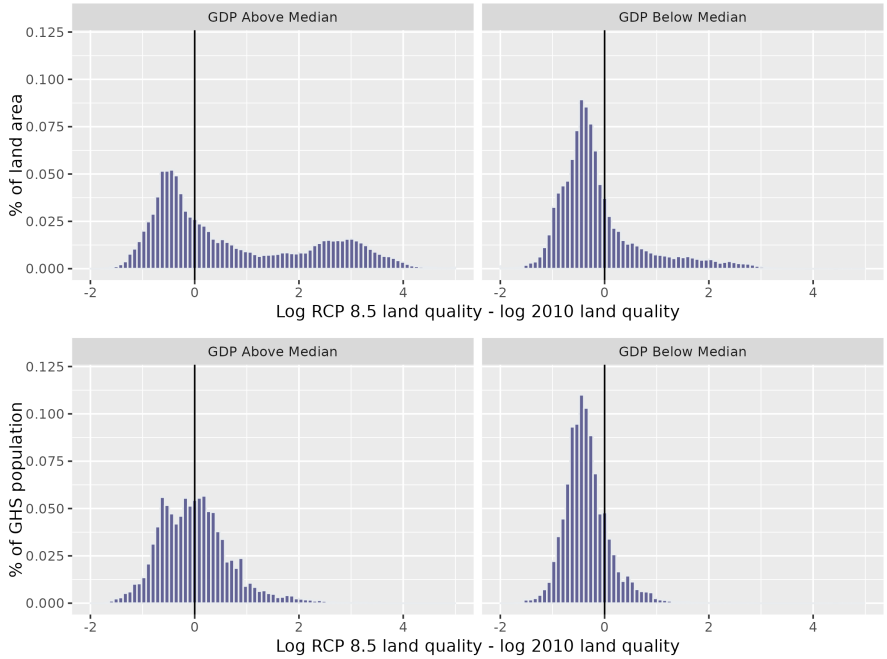

Notes: This figure depicts the distribution of cells in countries with above-median (left column) and below-median (right column) GDP in 2010. The histograms in the top row weight cells by their share of total land area in their respective country group; the horizontal axis is censored at -2 and 5. The histograms in the bottom row weight cells by their share of total GHS population in their respective country group; the horizontal axis is censored at -2 and 5.

To characterize global and regional impacts of climate change more formally, we define Average Location Quality (ALQ) of region r. We consider both area-weighted and population-weighted versions of this measure:

Area weighted:

$$ALQ_{r,t} = \sum_{i \in r} \hat{Q}_{i,r,t} \frac{Z_{i,r}}{Z_r} \tag{6}$$

Population weighted:

$$ALQ_{r,t} = \sum_{i \in r} \hat{Q}_{i,r,t} \frac{L_{i,r,2010}}{L_{r,2010}} \tag{7}$$

A region can be a province, a country, a continent or the world. The change in area-weighted ALQ measures the overall impact of climate change on a region, while

the change in population-weighted ALQ focuses on how quality will change in the places where people currently live. In Section 5 we discuss the assumptions regarding labor mobility and unobserved location attributes that justify using one or the other of these measures as a starting point in assessing the impact of climate change.

Appendix table E1 reports world- and continent-level $ALQs$ in 2010, using both weighting schemes. As would be expected, population-weighted ALQ, globally or in any region, is far higher than area-weighted ALQ, given that people disproportionately live in higher-quality areas. The table also reports projected $ALQs$ in 2100 for the four RCP emissions scenarios. Under RCP 8.5, world average location quality increases by 10% using area weights, but falls by 11% using population weights. Under either weighting scheme, the continent with the biggest gain is Europe (which includes all of Russia) and the one with the biggest loss is Africa.

4.2 Country-Level Results

Figure 3 shows that there is a strong relationship between countries' current levels of GDP per capita and projected changes in (area-weighted) location quality. Among countries with below-median GDP per capita, the average expected change in area-weighted location quality under RCP 8.5 is -25%; for those in the top half, the average is 51%. There is a good deal of variation among the richer countries, with some, such as Israel, Portugal, Greece, and the Gulf states doing poorly, while the Nordic countries, Japan, and New Zealand as well as Russia and Canada all do well. By contrast, among poor countries the projection is almost universally bad, with a few exceptions such as Mongolia, Tajikistan, and Moldova.

Taken by itself, this strong relationship between current income and expected effects of climate change on location quality would be a force pushing toward increased inequality among countries. If we look at population-weighted location quality, the average expected change remains at -25% for countries with below-median GDP per capita, while for the top half the increase in location quality shrinks dramatically to 25%. This suggests that increases to location quality in countries projected to benefit overall are concentrated in sparsely populated cells. Internal migration will thus play a large role in determining whether actual gains are realized from these changes.

4.2.1 Population Growth

The economic effects of climate change that we consider are expected to operate via a decline in the ability of the physical environment to provide support for the people

Figure 3: 2010 GDP and Future *ALQ* Changes

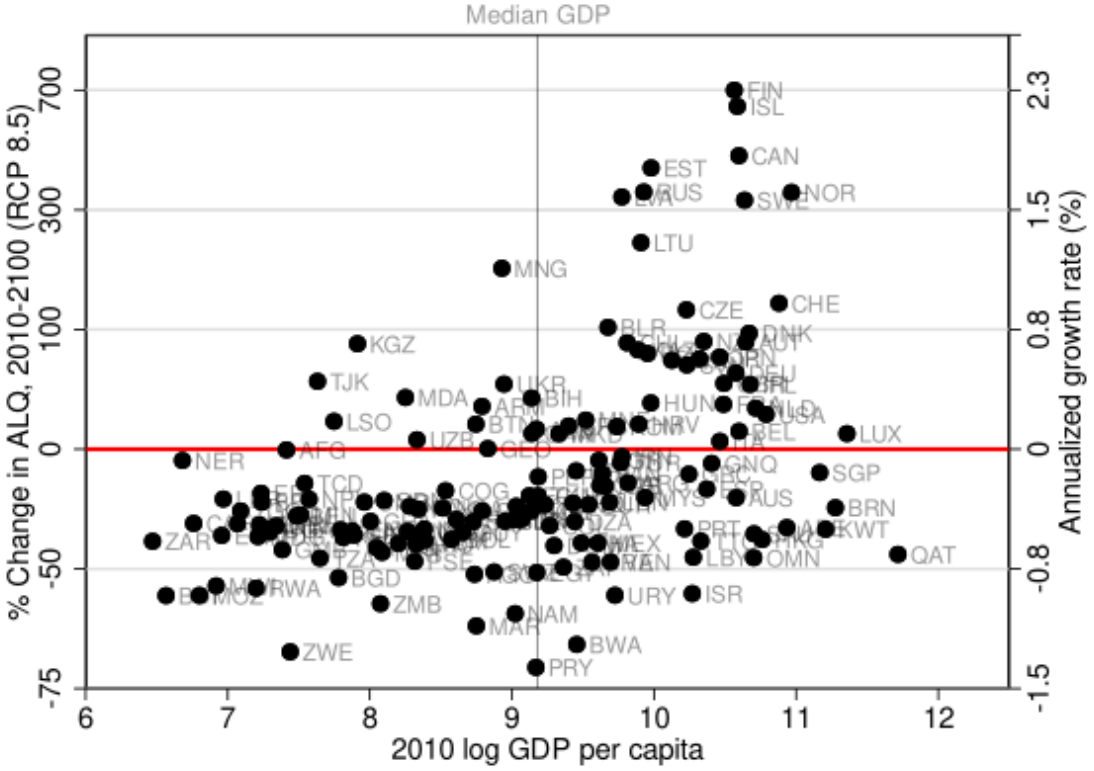

Note: Figure plots the percentage change in baseline area-weighted *ALQ* from 2010 to 2100 in RCP 8.5 in log scale against log 2010 GDP for the 156 countries with both values.

who live in it. A moment's thought suggests that another contributor to this problem is changes in the number of people. To a first approximation, we would expect a decline in location quality by 50%, holding constant the number of people living on it, to have the same economic effect as a doubling of the number of people, holding location quality constant.

Assessing this requires projections of future population. Unlike changes in *ALQ*, these are available only at the level of countries, not grid cells. We use population projections from the United Nations Population Division (United Nations, 2019). The UN provides a central forecast (the medium variant) as well as a range of probabilistic forecasts for each country. In this section, we use the medium variant projection for the year 2100, while in Section 6.4 we explore the full probabilistic range.

Figure 4 shows the relationship between current GDP per capita and expected population growth between 2010 and 2100 in the UN medium projection. The neg-

Figure 4: 2010 GDP and Future Population Growth

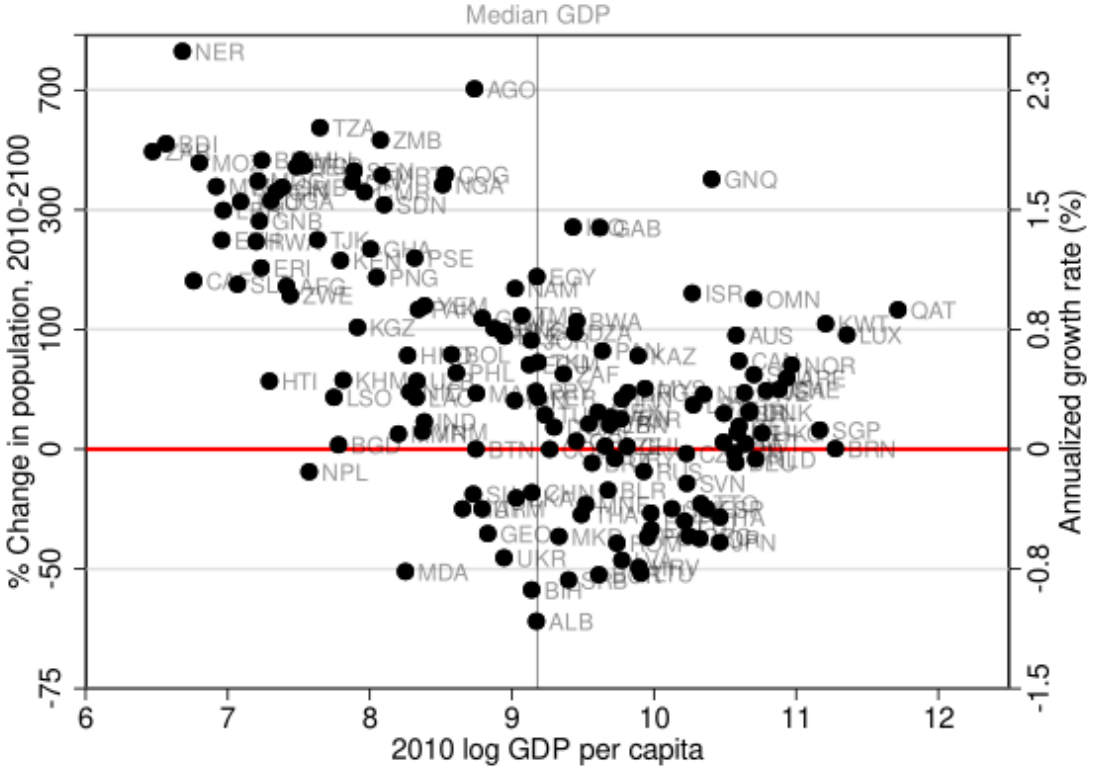

Note: Figure plots the percentage change in population from 2010 to 2100 in the U.N. medium variant projection using log scale against log 2010 GDP for the 156 countries with both values.

ative relationship is even more pronounced than the positive relationship between current GDP and expected changes in location quality shown in Figure 4. Many wealthy and middle income countries have negative projected population growth, and among the wealthy countries, those that do have positive projected growth generally have projected values of less than half a percent per year. The exceptions are mostly oil producers. By contrast, there are a significant number of poor countries where expected growth over this 90-year period is more than one percent per year, and many with expected growth near 1.5%.

We now turn to formally comparing the effects of expected population growth and climate change on economic growth.

5 Mapping Location Quality Changes and Population Growth into Income: Methodology

Changes in location quality and in the size of the population both act to change the degree of population pressure on natural resources. Following the existing literature on damage functions, our goal is to construct a quantitative measure of how income per capita in countries would differ in 2100 as a result of these changes, from what it would have been in their absence. Although the damage function approach is much more commonly applied in the case of climate change than in the case of population, we show that the two effects can be treated in parallel.

To measure the impacts of climate change and population growth we consider the comparison of specified baseline and alternative scenarios. Let $X_{i,base}$ and $X_{i,alt}$ be the 2100 values of quality-adjusted land in grid cell i under these two scenarios, with $L_{i,base}$ and $L_{i,alt}$ defined analogously. The choice of what baseline and alternative values to use will depend on the scenario being addressed.

We analyze the data for these scenarios in a simple Solow-type growth model. The model assesses how the relative capital to output ratio along steady state paths is affected by different scenarios, in a context where there are country specific saving, technological change, and depreciation rates that stay the same across scenarios. Details are in Appendix G. How the capital to output ratio changes is one, as it turns out minor element of determining how relative production per person for a country differs across scenarios in 2100 in the equations to follow.

The grid cell production function is (1) from above, substituting in the definition of quality adjusted land, $X_i = Z_i Q_i$:

$$Y_i = X_i^{\phi} K_i^{\alpha} (eL_i)^{1-\alpha-\phi}, \tag{8}$$

We suppress the country subscript when there is no ambiguity. e is productivity that is the same throughout a country. We do not explicitly include human capital, but one can think of this as being incorporated into the productivity term.

We need to aggregate from this grid cell production term into a national output equation. To do so, we assume that capital is perfectly mobile, so that the marginal product of capital is equalized across grid cells. It is simple to show that this leads to the capital-output ratio of each grid cell equaling the nationwide capital-output

ratio. That is,

$$\frac{K_i}{Y_i} = \frac{K}{Y}, \tag{9}$$

where K and Y are national magnitudes. We use equation (9) to write (8) as

$$Y_i = L_i \Big(\frac{X_i}{L_i}\Big)^{\phi/(1-\alpha)} \Big(\frac{K}{Y}\Big)^{\alpha/(1-\alpha)} e^{(1-\alpha-\phi)/(1-\alpha)}. \tag{10}$$

5.1 Labor Mobility

As shown above, climate change will have heterogeneous effects within countries. The extent to which this heterogeneity of climate impacts matters for aggregate output in a country depends on two factors. The first is the degree to which the spatial distribution of population can change in response to climate, which we refer to as labor mobility. The second is the empirical relationship between where population is located in the period prior to climate change, on the one hand, and the spatial distribution of climate impacts, on the other. This second factor is captured in the measure of population-weighted change in ALQ that we presented above.

We consider three cases. In the first ("perfect mobility"), population is assumed to be distributed in a manner that equalizes the average product of labor across grid cells in both the present and the future. In this case the distribution of land qualities within a country turns out to be irrelevant; all that matters is a country's total quality-adjusted area. The change in this area is captured by the area-weighted change in ALQ that we constructed above.

An issue with the approach in the perfect mobility case is that the observed distribution of population in the initial period does not match the distribution predicted by our location quality measure. In the second case we address this issue by assuming that there are location-specific attributes that produce this residual variation in density, and further that these attributes will persist into the future. We thus call this case "perfect mobility with unmeasured quality."

Comparing the first and second cases gives insight into the importance of the heterogeneity of climate impacts. Some countries will turn out to be lucky in the sense that they have an unexpected concentration of population (beyond what would be predicted by pure geography) in regions that are expected to do unusually well as a result of climate change, while other countries have bad luck in this respect.

The third case allows us to consider the importance of population mobility in response to heterogeneity of climate change impacts within a country. The starting point is the same as in the second case. Specifically, we assume that there are unmeasured location-specific characteristics that, along with observed geographic attributes, perfectly explain the distribution of population in the initial period. Unlike the second case, however, we then assume that the relative populations of grid cells remain fixed over time. We call this case "no mobility going forward." Comparing the second and third cases, we can characterize the benefit of internal migration as a form of adaptation.

5.2 Perfect Mobility

Equating the marginal product of labor across grid cells within a country implies that the ratio of labor to quality-adjusted land is equalized across grid cells, and is equal to this same ratio measured at the national level:

$$\frac{L_i}{X_i} = \frac{L}{X}. \tag{11}$$

Substituting equation (11) into (10), grid square output per worker is

$$\frac{Y_i}{L_i} = \frac{Y}{L} = \left(\frac{X}{L}\right)^{\phi/(1-\alpha)} \left(\frac{K}{Y}\right)^{\alpha/(1-\alpha)} e^{(1-\alpha-\phi)/(1-\alpha)}. \tag{12}$$

Through labor and capital mobility, grid-cell level output per capita is a function of national magnitudes and thus is constant across grid cells. We can aggregate labor, quality-adjusted land, and capital to the country level in each period by simply summing. This corresponds to what we called the area-weighted case in calculating changes in location quality above.

Using (12) we can compare output per capita in the baseline and alternative scenarios:

$$\frac{\left(\frac{Y}{L}\right)_{alt}}{\left(\frac{Y}{L}\right)_{base}} = \left(\frac{\sum_i exp(x_{i,alt}\hat{\beta})Z_i}{\sum_i exp(x_{i,base}\hat{\beta})Z_i}\right)^{\frac{\phi}{1-\alpha}} \left(\frac{L_{alt}}{L_{base}}\right)^{\frac{-\phi}{1-\alpha}} \left(\frac{(K/Y)_{alt}}{(K/Y)_{base}}\right)^{\frac{\alpha}{1-\alpha}}. \tag{13}$$

In the language of the climate change literature, (13) is one minus climate damages. Of the three terms on the right hand side of the equation, the first two have obvious interpretations in terms of population pressure on natural resources: output

in the alternative case is lower than in the base case to the extent that location quality in the alternative is lower or that population is higher than in the base. As noted earlier, the third term on the right hand side of (13) is analyzed in Appendix G. Specifically, we derive this term and discuss its magnitude for all three of the labor mobility cases that we consider, in the Solow-style model we employ. We show that location quality degradation (i.e. $\hat{X}_{alt} < \hat{X}_{base}$) and lower population growth (i.e. $\hat{L}_{alt} < \hat{L}_{base}$) both raise the capital/output ratio in the alternative case relative to the base case. We also show that in practice this term is always quite close to one, and thus of little quantitative importance.

5.3 Perfect Mobility with Unmeasured Quality

In this case, we continue to assume that labor is perfectly mobile in the present and the future. However, rather than assuming, as in the previous case, that year 2010 population is distributed according to our fitted measure of location quality, we instead assume that there is an unobserved dimension of location quality that explains the current population distribution.

Specifically, we define the multiplicative residual ϵ_i that makes our equation for location quality fit the distribution of population in every country exactly:

$$\frac{L_i}{Z_i} = \exp(\hat{C}_c + x_i\hat{\beta})\epsilon_i. \tag{14}$$

We assume that this residual ϵ_i represents unmeasured location quality, and that it is time-invariant. This assumption is meant to capture unmeasured aspects of locations that are either time-invariant or highly persistent which give rise to grid squares with unusually high and sustained agglomeration. These could be special geographic features such as a particular deep natural harbor. They could also represent the accumulation of highly durable public infrastructure and social capital that historical urban agglomerations enjoy. Because of these stocks, large urban agglomerations persist in their relative size rankings over decades and centuries.[12] This formulation tries to capture that aspect of location quality.

Our new measure of location quality for every grid square is then the fitted value from this equation, suppressing the country fixed effect:

[12]See Eaton and Eckstein (1997), Black and Henderson (2003), and Duranton (2007).

$$\hat{Q}_{i,c} = \exp(x_i\hat{\beta})\epsilon_i. \tag{15}$$

The change in aggregate location quality is now

$$\left(\frac{X_{alt}}{X_{base}}\right) = \frac{\sum_i exp(x_{i,alt}\hat{\beta})\epsilon_i Z_i}{\sum_i exp(x_{i,base}\hat{\beta})\epsilon_i Z_i} \tag{16}$$

This in turn can be rewritten as

$$\left(\frac{X_{alt}}{X_{base}}\right) = \sum_i \left(\frac{L_{i,base}}{L_{base}}\right) \frac{exp(x_{i,alt}\hat{\beta})}{exp(x_{i,base}\hat{\beta})} \tag{17}$$

This is a weighted average of grid-cell specific changes in location quality, where the weights are the population of each grid cell in the baseline.

Equation (13) can now be rewritten as

$$\frac{\left(\frac{Y}{L}\right)_{alt}}{\left(\frac{Y}{L}\right)_{base}} = \left(\sum_i \left(\frac{L_{i,base}}{L_{base}}\right)\frac{exp(x_{i,alt}\hat{\beta})}{exp(x_{i,base}\hat{\beta})}\right)^{\frac{\phi}{1-\alpha}}\left(\frac{L_{alt}}{L_{base}}\right)^{\frac{-\phi}{1-\alpha}}\left(\frac{(K/Y)_{alt}}{(K/Y)_{base}}\right)^{\frac{\alpha}{1-\alpha}}. \tag{18}$$

The second term of (18) is the same as in equation (13). The third term is similar to that in (13) and is given in Appendix G. The first term differs, in that for the case of perfect mobility (equation (13)), location quality is aggregated by using area weights, while for the case of perfect mobility with unobserved quality (equation (18)), changes in location quality are aggregated using population weights.

5.4 No Mobility Going Forward

We present one more case, which is useful for demonstrating the role of mobility in mitigating the effects of climate change. Our starting point is the same as in the previous case, which is specifically that the observed population distribution in 2010 is such that the average product of labor is equalized across grid cells, with unobserved quality ϵ_i explaining the deviation of the observed distribution from what would be explained by observed location characteristics and our estimated coefficient vector $\hat{\beta}$. Unlike the previous case, however, we now assume that there is no population mobility in the face of heterogeneous impacts from climate change. More specifically, we assume that population in each grid cell in a country grows (or shrinks) at the

same rate:

$$\frac{L_{i,alt}}{L_{i,base}} = \frac{L_{alt}}{L_{base}} \tag{19}$$

Unlike the previous two cases, output per worker will not be equalized across grid squares in the alternative case.

Aggregate output per worker is given by summing equation (10):

$$\frac{\left(\frac{Y}{L}\right)_{alt}}{\left(\frac{Y}{L}\right)_{base}} = \left(\frac{L_{base}}{L_{alt}}\right)\left(\frac{(K/Y)_{alt}}{(K/Y)_{base}}\right)^{\frac{\alpha}{1-\alpha}} \frac{\sum_i L_{i,alt}^{\frac{1-\alpha-\phi}{1-\alpha}} [exp(x_{i,alt}\hat{\beta}) Z_i \epsilon_i]^{\frac{\phi}{1-\alpha}}}{\sum_i L_{i,base}^{\frac{1-\alpha-\phi}{1-\alpha}} [exp(x_{i,base}\hat{\beta}) Z_i \epsilon_i]^{\frac{\phi}{1-\alpha}}}. \tag{20}$$

This can be rewritten (skipping several steps) as

$$\frac{\left(\frac{Y}{L}\right)_{alt}}{\left(\frac{Y}{L}\right)_{base}} = \left(\sum_i \frac{L_{i,base}}{L_{base}} \left(\frac{exp(x_{i,alt}\hat{\beta})}{exp(x_{i,base}\hat{\beta})}\right)^{\frac{\phi}{1-\alpha}}\right)\left(\frac{L_{alt}}{L_{base}}\right)^{\frac{-\phi}{1-\alpha}}\left(\frac{(K/Y)_{alt}}{(K/Y)_{base}}\right)^{\frac{\alpha}{1-\alpha}}. \tag{21}$$

The second term of (21) is the same as in equations (13) and (18). The third term is similar to that in (13) and is given in Appendix G. The first term, representing the effect of the change in location quality, looks almost the same as (18), except that the change in quality for each grid cell is raised to a power before being summed rather than after.

6 Mapping Location Quality Changes and Population Growth into Income: Results

Equations (13), (18), and (21) provide parallel structures for estimating the effects of projected climate change and population growth under different assumptions about future labor mobility.

We start by examining the pure effect of climate change. After this, we examine the combined effects of climate change and population growth. For brevity we don't look at effects of different population growth scenarios, absent climate change.

To apply this framework, we need values for the production function parameters. A commonly used estimate for the natural resource share in production, ϕ, is 0.25.

While this is probably too high for wealthy countries, we view it as reasonable for poorer countries, which are mostly reliant on local resources.[13] If we assume a one-third share for capital among inputs other than natural resources, we get $\alpha = 0.25$. We further assume that the annual growth rate of productivity in the Solow model, $\hat{e}$, is 1% and depreciation, δ, is 5%. However, these last two parameters are only relevant for the calculation of the term describing the change in the K/Y ratio in equations (13), (18), and (21). Appendix Table G1 shows that this term contributes little to variation across countries in projected climate impacts, and is insensitive to the choice of $\hat{e}$.

6.1 Climate Change Effects

To assess the pure effect of climate change, we project outcomes for 2100 under different climate scenarios, allowing for the same expected population growth. For all three equations, we set $X_{i,Base}$ equal to its 2010 value and $X_{i,Alt}$ equal to its 2100 value for each specified climate scenario. We set L_{Base} and L_{Alt} equal to the UN's 2100 median population forecast.[14] Thus we are comparing balanced growth outcomes in 2100 under different climate scenarios holding population growth constant across scenarios.

Figure 5 shows our results graphically for RCP 8.5 under the perfect mobility assumption, i.e. equation (13). As expected, Nordic countries, Canada, and Russia gain while countries in or near the tropics typically lose. The largest income losses are in Paraguay (33%), followed by Zimbabwe (31%), Botswana (30%), and Morocco (27%). On the other end, GDP per capita is 92% and 59% above baseline in Finland and Russia. In Appendix Figure D1, we look at these climate impacts on GDP per capita in the case of below-median income countries, if we estimate equation (4) using a sample of grid squares solely from countries with below-median income and then solely from countries with above-median income. The figure shows the results are highly correlated with the base case.

Of the three sets of results, impacts generated under the assumption of per-

[13] Hansen and Prescott (2002) assume a value of the fixed factor share of 30% for preindustrial economies. Cruz and Rossi-Hansberg (forthcoming) use 0.20 as the natural resource share in production, although they also allow for a congestion cost in amenities. Ashraf et al. (2009), using data from Caselli and Feyrer (2007), calculate resources shares in national income that are as high as 25% in many poor countries, and exceed 30% in a few.

[14] In Section 7, when aggregating to the world, we consider two alternative sets of population projections.

Figure 5: Country-Level Impacts from Climate Change with Perfect Mobility

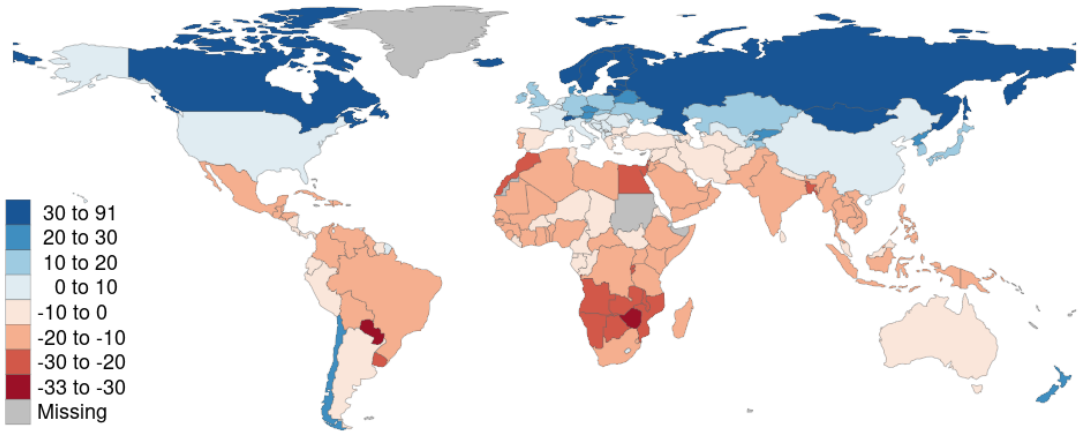

Notes: Countries are binned by the difference between GDP per capita under RCP 8.5 and no climate change under the assumption of perfectly mobile labor.

fect mobility with unmeasured quality are the most comparable to projections using population-weighted changes in climate such as Burke et al. (2015a), which is probably the best known application of the panel-weather approach to estimating the impact of climate. [15] Comparing the RCP 8.5 projections (expressed in percent changes) from Burke et al. (2015a) with ours, we find that the correlation is 0.76. However, the magnitudes are very different. In the Burke et al. (2015a) projection, 20 counties suffer damage to GDP per capita of more than 90%, and 72 countries more than 80%. By contrast, our maximum loss is 31%. Similarly, in Burke et al. (2015a) climate change increases GDP per capita in four countries by more than 300%, while in our estimates the biggest increase is 82%.

Given the relatively small magnitude of the estimated climate damages that we present, it is especially important to discuss channels of climate damage that are omitted from our analysis. The two most important of these are sea level rise and extreme weather events. In both cases, the existing literature is relatively thin. Newman and Noy (2021) examine the economic impact of extreme weather events (primarily storms, heatwaves, and floods). For the period 2000-2019, they estimate that the extreme events induced by climate change produced damages averaging $143 billion per year, or roughly 0.25% of world GDP. Prospectively, in the DICE-2023 model

[15] Country-level impacts calculated using all three assumptions about labor mobility for all four RCPs are available in the online supplement. Country-level projected per capita GDP with and without climate change from Burke et al. (2015a) is provided here.

(Barrage and Nordhaus, 2023), the authors survey existing literature to create an ad-hoc adjustment for the expected flow of climate damages due to extreme weather events, loss of biodiversity, and other channels omitted from their (and our) analysis. In the case of warming of 3 degrees C, these adjustments total 0.5% of world GDP. MacManus et al. (2021) estimate that in 2015, between 3.8% and 9.5% of the world's population lived in Low Elevation Coastal Zones less than 5 meters above sea level. IPCC projections (assessment report 6) indicate that under a very high emission scenario, roughly comparable to RCP 8.5, average sea level rise by the year 2100 would be approximately one meter, although with significant spatial variation. Desmet (2021) estimate that under RCP 8.5, 0.79% of the world population will be displaced due to inundation from sea level rise. GDP losses from this inundation peak in the year 2151 at 0.71% of world GDP.

6.1.1 Alternative Labor Mobility Assumptions

In Figure 6 we compare country-level outcomes across the three mobility assumptions. In panel (a), we first compare the effects under perfect mobility assumptions to those under assumptions of perfect mobility with unmeasured quality. It is immediately apparent that, while the two sets of predictions are highly correlated, points are scattered on both sides of the 45 degree line. These deviations from the 45 degree line result from the unevenness of climate change impacts within a country and the extent to which particularly strong impacts take place in regions that are more or less populated than would be expected based on current location quality. Countries whose location quality increases the most in currently sparsely populated areas see far smaller gains to output when unmeasured quality is taken into account; this is the case for Canada, Norway, and Iceland. The reverse holds true for countries like Peru and Bolivia, where for historical reasons many people live in mountainous areas and climate changes favor the places where economic activity is clustered. The estimated overall effect on GDP per capita for Bolivia is -15% under the perfect mobility assumption and 20% under the perfect mobility with unmeasured quality assumption.[16]

Panel (b) likewise compares results assuming unmeasured quality and past perfect mobility with either perfect mobility or no mobility going forward. This captures the

[16]The vertical distance of each country from the 45 degree line in panel (a) of Figure 6 is closely related to the difference between its area-weighted and population-weighted change in ALQ discussed above (correlation coefficient of 0.63).

mitigating influence of mobility on climate change effects. All countries are below the 45 degree line, because impacts under no mobility will always be more negative than with perfect mobility. However, this downward pressure is small in most countries.[17]

While the deviations from the 45 degree line in Figure 6 are interesting objects for study, we think that the most notable message from this analysis is that for most countries, and certainly for most countries that are expected to suffer negative consequences from climate change, the assumption made regarding labor mobility makes little difference for the projected effect of climate change on GDP per capita. For that reason, in the rest of this section we present results for the perfect mobility case, although the full set of results for alternate cases are given in the online supplement.

Below, in Section 7, we calculate the world damage function by aggregating these country-level damages of climate change using projections of country-level GDP in 2100.

6.2 Combined Impacts from Climate Change and Population Growth

In this section we look at the combined effects of climate change and population growth. In the next one, we then compare their relative magnitudes. Concretely, we will set $X_{i,Base}$ and $L_{i,Base}$ to their 2010 values and then use different combinations of projections to 2100 for $X_{i,Alt}$ and $L_{i,Alt}$.

Figure 7 shows the relationship between GDP per capita and the combined impacts from climate change under RCP 8.5 and population growth under the UN medium projection. Because countries that are projected to suffer land degradation from climate change tend to also be the ones where population is growing fastest, the size of impacts in Figure 7 tend to be much larger than those in Figure 5 where population growth does not differ between the base and alternative cases. Many countries, mostly poorer ones, experience losses well over 35% and many even over 50% of GDP per capita with combined population growth and climate deterioration. For example, Angola is projected to experience an impact of -20.4% from climate change alone, but an impact of -63.4% from climate change combined with population growth. The

[17] We can also project the size of climate-induced migration within countries by comparing the implied population distributions over grid cells in the year 2100 in these two cases. Worldwide, 13.5% of the population would be living in a different grid square under the full mobility assumption compared to the assumption of no mobility going forward.

Figure 6: Comparisons of Country-Level Impacts from Climate Change

(a) Perfect Mobility vs. Perfect Mobility with Unmeasured Quality

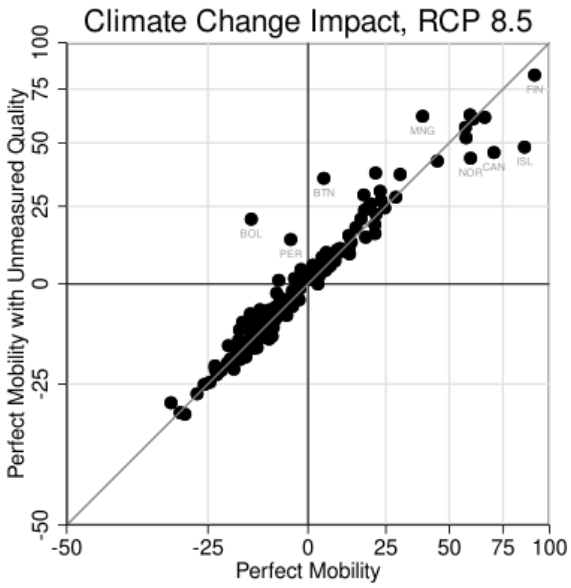

Note: Figure compares the percentage impact of climate change in 2100 under perfect mobility assumptions against that under perfect mobility with unmeasured quality. RCP 8.5 and the U.N. medium variant population projection are used for each case; 164 countries are depicted.

(b) Unmeasured Quality: Perfect Mobility vs. No Mobility Going Forward

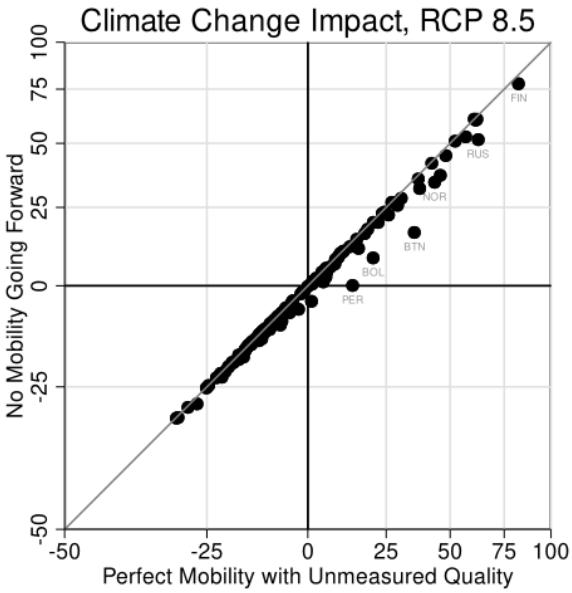

Note: Figure compares the percentage impact of climate change in 2100 under assumptions of perfect mobility with unmeasured quality against that of no mobility going forward. RCP 8.5 and the U.N. medium variant population projection are used for each case; 164 countries are depicted.

cross-country correlation between current log GDP of per capita and the projected impact of climate alone is 0.42, while the correlation between current log GDP and the the projected combined effects of climate and population is 0.55.

Figure 7: Impacts from Climate Change and Population Growth

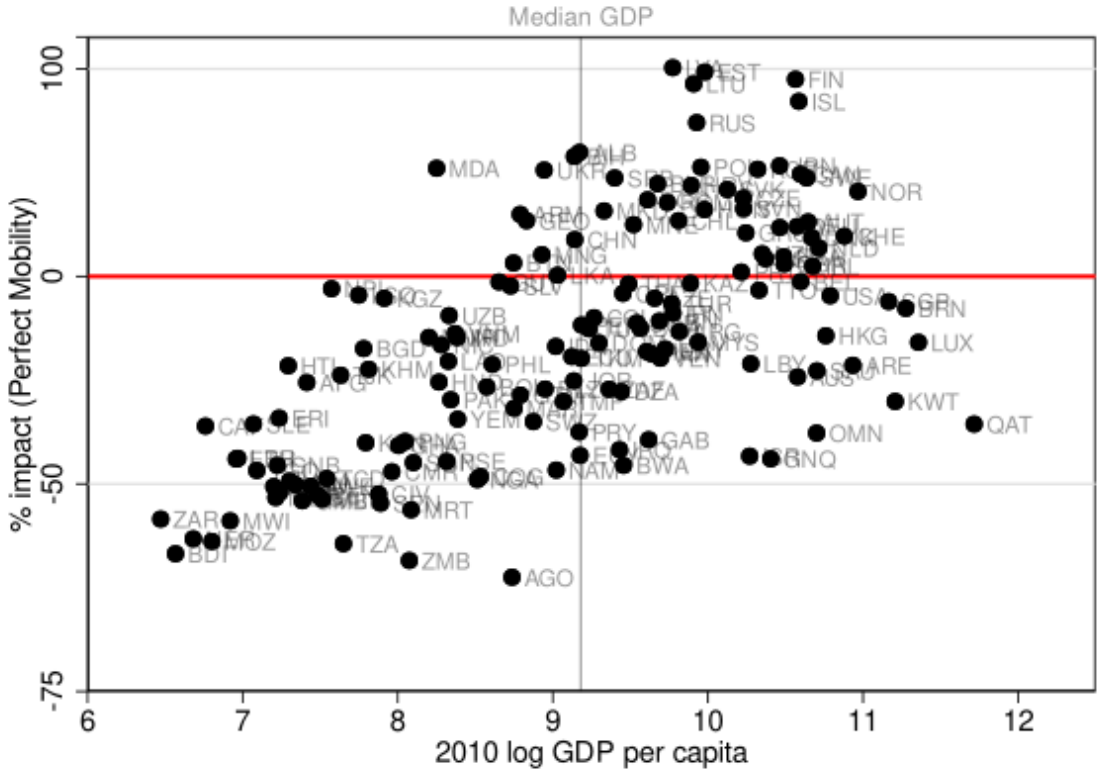

Note: The vertical axis plots the percentage impact of climate change in 2100 using RCP 8.5 and the U.N. medium variant population projection under perfect mobility assumptions in log scale. The horizontal axis plots log 2010 GDP. 156 countries are shown.

6.3 Relative Importance of Climate Change and Population Growth

The analysis above naturally raises the question of the relative magnitude of effects from climate change and population growth. In equation (13), we want to compare the first term, $\left(\frac{\sum_i exp(x_{i,alt}\hat{\beta})Z_i}{\sum_i exp(x_{i,base}\hat{\beta})Z_i}\right)^{\frac{\phi}{1-\alpha}}$, to the second, $\left(\frac{L_{alt}}{L_{base}}\right)^{\frac{-\phi}{1-\alpha}}$. However, a complete answer to this question is complicated by the fact that both of these effects enter the third term in equation (13). Fortunately, in practice, as noted above and in Appendix Table G1, this third term is of relatively minor importance.

Figure 8 looks at how these two terms vary across countries. Each country is represented by a dot, with red dots indicating countries with GDP per capita below the median. The horizontal axis measures the first term (i.e. the impact of location quality change on GDP per capita) and the vertical axis measures the second (impact of population change on GDP per capita).

Figure 8: Climate Change and Population Impacts

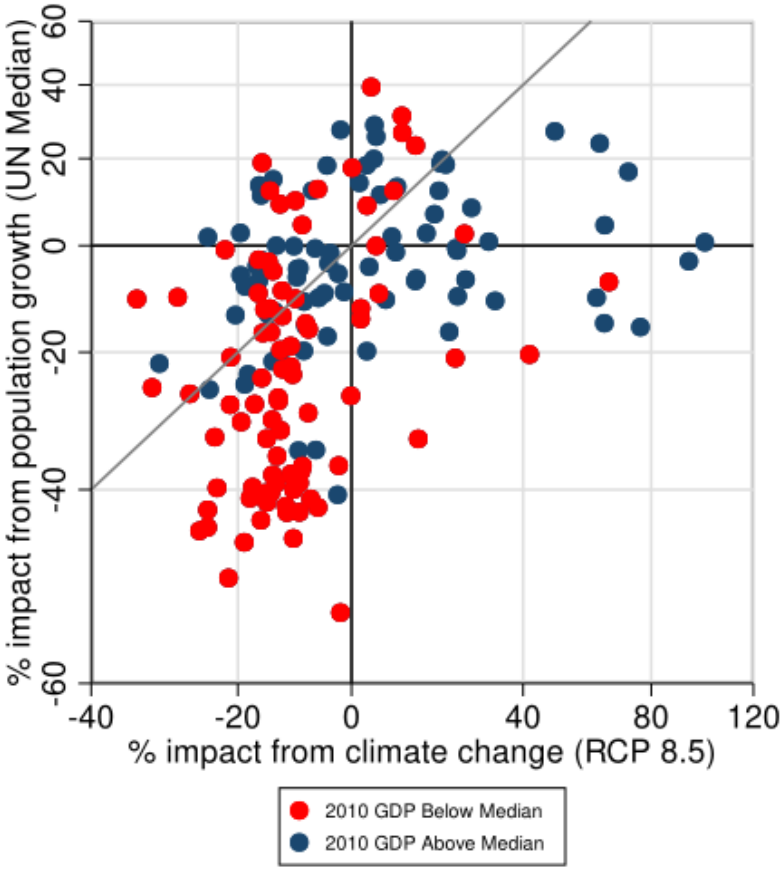

Note: Figure compares the effect of the the second term in equation (13), which represents the impact of population growth, against the first term, which represents the impact of climate change in 2100. Impacts are calculated in percentages under perfect mobility assumption using RCP 8.5 and the U.N. medium variant population projection and plotted in log scale; 164 countries are shown.

Countries on the 45 degree line are those for which the impacts of changes in location quality and population growth are equal. Countries below the 45 degree line have either more positive or less negative impacts of climate change than population growth, and vice versa for those above. Those negatively affected by climate change are to the left of the vertical line at 0 and are mostly low income countries, while

those to the right of that line are disproportionately high income. Similarly looking at the horizontal line at 0, those countries negatively affected by population growth are disproportionately low income countries. That is, low income countries tend to suffer losses from both population growth and climate change. Quantitatively, climate losses are all under 35%, while many countries have losses from population growth that are in the 40–50% range. These countries are mostly poor and agricultural—that is to say, more prone to suffer from congestion and declining location quality, and in a worse position to deal with the consequences of these changes. Finally we note that the gains from climate change tend to exceed gains from population decline.

Figure 8 makes clear that for most countries projected to experience high levels of damage from climate and population growth taken together, the biggest source of that damage is population growth. There are a few countries such as Paraguay and Morocco where effects from projected population increases are much smaller than those from projected declines in location quality. But for the majority of countries, the major culprit is population growth. To give a typical example, in Tanzania, the impact of declining location quality is projected to be -19%, while the impact due to rising population is projected to be -46%.

It is worth recalling that all of this analysis is done using RCP 8.5, the most extreme climate scenario. As we explore further below, using projections from a less dire climate projection further elevates the relative importance of population growth as a driver of damages.

6.4 Variation Across Projections

In the analysis above, we focused on RCP 8.5, the most extreme of the four climate scenarios, along with the UN medium population projections. The fact that organizations like the IPCC and the UN produce ranges of scenarios is indicative of the uncertainty regarding these projections. A natural implication of this is that one can learn something about the range of possible outcomes by looking at the range of scenarios.

In the case of the UN, they explicitly state that:

> In projecting future levels of fertility and mortality, probabilistic methods were used to reflect the uncertainty of the projections based on the historical variability of changes in each variable. The method takes into account the past experience of each country, while also reflecting uncertainty about

future changes based on the past experience of other countries under similar conditions. The medium-variant projection corresponds to the median of several thousand distinct trajectories of each demographic component derived using the probabilistic model of the variability in changes over time. Prediction intervals reflect the spread in the distribution of outcomes across the projected trajectories and thus provide an assessment of the uncertainty inherent in the medium-variant projection.[18]

Unlike the population projections, there are no official probabilities assigned to the different RCPs used to assess the effects of changing climate, nor is there any claim that the actual path of climate change will fall within the span of the four commonly used RCPs. Rennert et al. (2022) report a state-of-the-art attempt to address this gap by pairing a set of probabilistic projections of carbon emissions with a simplified climate model.[19] In their model, RCP 2.6, 4.5, 6.0, and 8.5 are in the 2.4th, 20th, 90th, and 99th percentiles, respectively, suggesting that a 95% prediction interval is narrower than the gap between RCPs 2.6 and 8.5 that we report.

In conducting this analysis, we restrict ourselves to looking at individual countries, rather than trying to aggregate to the level of the world as a whole. We start with an example for a single country, India. Table 1 shows the percentage change in GDP per capita in 2100, relative to a scenario where population and climate are unchanged. We consider four climate scenarios and five population scenarios, all under perfect population mobility.

Using the median UN forecast, India's GDP will be around 18% lower in RCP 8.5 than if both population and climate had remained the same. The main result in the table, however, is that moving across climate scenarios has a much smaller effect on the expected change in GDP per capita than does moving across population scenarios. For any given population scenario, the difference between the total impact of climate and population on GDP, comparing the most extreme climate scenarios, is about 10

[18] https://population.un.org/wpp2019/DefinitionOfProjectionVariants

[19] Rennert et al. (2022) pair Resources for the Future Socioeconomic Projections (RFFSP) with the Finite Amplitude Impulse Response model (FaIR; Millar et al., 2017). Unlike global climate models such as GFDL, which comprehensively model climate systems with a computationally expensive set of equations, the FaIR model is a simplified impulse-response model that tries to capture the increase in atmospheric concentrations of carbon and the resulting change in global mean temperature from an influx of carbon emissions. FaIR translates the probabilistic carbon emission projections generated by RFFSP into carbon concentration paths, from which we can calculate the percentile of the RCP carbon concentrations in 2100.

percentage points. By contrast, for a fixed climate scenario, the range of impacts on GDP comparing the highest to the lowest population growth scenarios is roughly 30 percentage points. Even comparing the 10th to the 90th percentile population growth number gives a range of impacts on GDP per capita of roughly 20 percentage points.

Table 1: Impact of Climate Change and Population on GDP per Capita in India

	RCP	**2.6**	**4.5**	**6.0**	**8.5**
	$\%\Delta QAA$	**-15**	**-16**	**-29**	**-37**
%ile	$\%\Delta Pop.$				
2.5	**-28**	8	7	2	-2
10	**-14**	1	1	-5	-8
50	**17**	-11	-11	-15	-18
90	**52**	-19	-19	-23	-26
97.5	**77**	-23	-23	-27	-30

Note: The numbers in bold in the first numerical column provide the percent change in population from 2010 to 2100 for each of the five population projections provided by the UN. The bold numbers in the first numerical row provide the percent change in *ALQ* from 2010 to 2100 corresponding to each RCP. The 5×4 matrix provides the percent change to GDP per capita for each population projection-climate scenario pair according to equation (13). UN projections provide 80% and 95% prediction intervals. We treat the lower bound of the 80% prediction interval as the 10th percentile of distribution of projections, and similarly for other bounds.

In the perfect mobility case, we can use equation (13) to separate out variation in climate change and population growth in the total impact. As before, we ignore the term representing the change in the K/Y ratio, which is very small.[20] Figure 9 expands this analysis graphically to look at 9 particularly interesting countries. Each country is represented by a colored rectangle. The horizontal dimension of the rectangle shows the range in projected impacts from location quality change (the first term in equation (13)), looking across all four RCPs. The vertical dimension of the rectangle is the range of the impact of population growth on GDP per capita (the second term of equation (13)), going from the 2.5th to the 97.5th probability percentile projections of the population in 2100.

As an illustrative example, for Malawi, the rectangle showing the range of GDP per capita losses is much taller than it is wide, indicating that there is less uncertainty regarding the effect of climate change than there is regarding the effect of population change. The rectangle for Malawi is also entirely in the lower-left quadrant (rising population, falling location quality), indicating that, within the range of these

[20]Values for country-level damages inclusive of this term under all RCPs and population scenarios can be found in the online supplement.

Figure 9: Range of Impacts from Climate Change and Population for Selected Countries

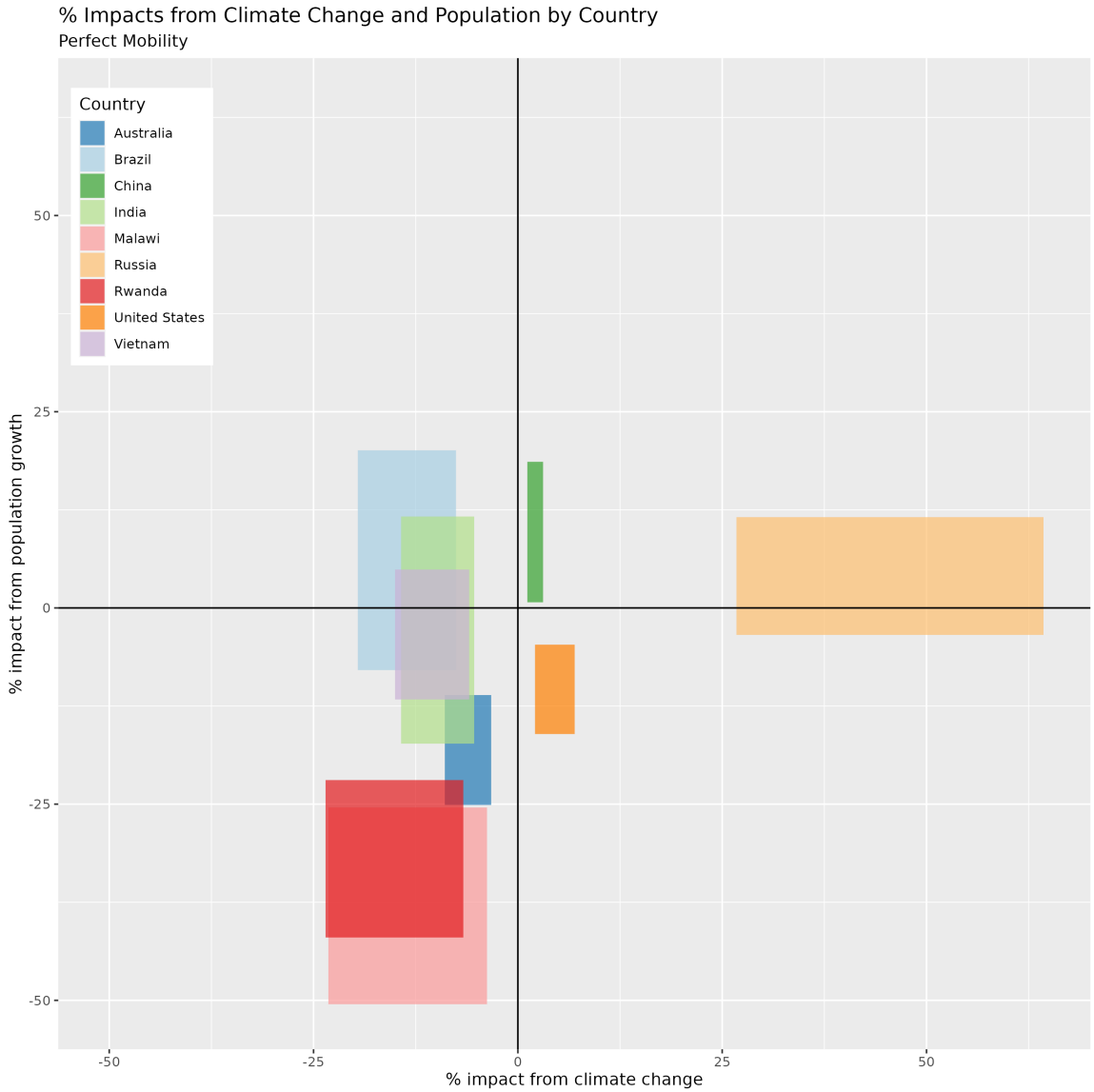

Note: This plot depicts the range of impacts on GDP, as percentage changes, across the four climate scenarios (horizontal axis) and the 2.5th to 97.5th percentile population scenarios (vertical axis), as derived from the first and second terms of equation (13).

estimates, all scenarios will lead to an increase in population pressure on quality-adjusted land. By contrast, the rectangle for Russia is wider than it is tall, i.e. there is more uncertainty about the effect of climate than about population. Russia also sits largely in the upper right quadrant, indicating that both forces will be pushing toward reduced population pressure on land.

Although we display only a limited number of countries in Figure 9 for illustrative purposes, looking over all poor countries there is a strong empirical regularity: not only is expected damage from population growth larger than expected damage from climate change, but variation in damage among population scenarios is also larger than variation in damage across climate scenarios. Among countries with 2010 GDP per capita below the median in our sample, 97% face larger uncertainty from population than from climate. Among countries with above-median GDP, the proportion is slightly lower at 81%.[21]

7 The World Damage Function and Cross-Country Inequality

In this section, we assess the damage from climate change at the world level. We have two motivations. First, a good deal of literature has estimated a world damage function from climate change, and we want to be able to compare our results to this literature. Second, we want to explicitly examine the role of climate change in impacting cross-country income inequality.

Conducting either of these exercises involves combining the country-level climate damages calculated in Section 6 with an additional piece of information: the *level* of total output in each country in 2100 in the absence of climate change. Our analysis thus far has not required estimates of these levels, but rather calculated percent losses or gains from whatever the level might be. We utilize two sources for projections of country-level output in the absence of climate change.

The first set of projections come from Shared Socioeconomic Pathways (SSPs), which are established and commonly employed scenarios for how the world economy might evolve in the absence of both climate change and climate mitigation or adaptation policies (O'Neill et al., 2014; Riahi et al., 2017). These pathways from the point of view of economists have a lot of issues and in many cases seem both inconsistent

[21]Results for all countries have been made available in the online supplement.

with known patterns in growth data and unrealistic (Welch, 2024). Nevertheless, given their wide usage, we show results for them here. The different pathways embed particular assumptions about technological change, population and economic growth, and cross-country income convergence, among other dimensions. For example, SSP 5 features the following: rapid income growth at the world level combined with a incredible decline in income gaps among countries, and world population peaking around the year 2060 and then declining to around 7 billion in 2100.[22] Using integrated assessment models, emissions can be generated for each SSP. We consider four specific pairs of SSPs and warming scenarios that align with RCPs.[23]

The second source of country-level output in the absence of climate change is Resources for the Future Socioeconomic Projections (RFF-SPs; Rennert et al., 2021, 2022), which for economists may seem more realistic. While SSPs provide comprehensive scenarios consistent with five established narratives, RFF-SPs combine expert surveys and statistical methods to generate sets of Monte-Carlo trajectories that contain world emission paths and corresponding country-level paths of population and income in the absence of climate change. From a sample of 100,000 such trajectories, we identify those with emission paths close to each RCP, and use these to weight country-level effects.[24]

Table 2 shows the damage function at the world level, which aggregates country losses weighted by their 2100 GDP in the absence of climate change from these two sources. Panel 2a uses the full sample of 156 countries, while panel 2b limits the sample to the 78 countries with below-median incomes in 2010. In each panel, columns under the SSP header identify the SSP scenario paired to each RCP and provide the relevant population, baseline world GDP, and climate impact. Climate impact is calculated as the weighted average of country-specific percentage changes in GDP under the particular SSP-RCP scenario assuming population mobility within

[22]Projections of population, urbanization, and GDP that quantify the narratives of the Shared Socioeconomic Pathways are available in a database hosted by the International Institute for Applied Systems Analysis (IIASA) Energy Program at `https://tntcat.iiasa.ac.at/SspDb`. We use the projections of the Organization for Economic Co-operation and Development (OECD; Dellink et al., 2017), considered the "illustrative" case. Population projections for each SSP are from Samir and Lutz (2017).

[23]IPCC Assessment Report 6 uses scenarios labeled SSPX-Y, where X is the SSP number and Y is the radiative forcing level in 2100 for the matched warming scenario. As discussed in Chen et al. (2023), these scenarios overlap with the trajectories described by RCPs but are not identical.

[24]We define proximate draws as those with 2100 global CO2 concentrations that fall within 2.5% of the RCP value. Emissions from the draws are translated to concentrations with the FaIR model.

countries as in equation (13). Because each RCP is linked to a sample of RFF-SP draws, columns under the RFF-SP header provide the means and standard deviations of the population, baseline world GDP, and climate impact as well as the sample size.

Table 2: 2100 Climate Change Impacts as Percentage of Aggregate GDP

(a) Full Sample

Scenario (RCP)	SSP				RFF-SP						
	2100 Base			%	2100 GDP		2100 Pop.		% Impact		
	SSP	GDP	Pop.	Impact	Mean	SD	Mean	SD	Mean	SD	N
2.6	1	565	6.87	-0.72	899	920	10.83	0.82	0.50	0.69	4309
4.5	2	538	8.98	-0.84	772	808	10.83	0.82	0.64	1.05	9590
6.0	4	353	9.25	-0.03	833	871	10.83	0.82	0.08	1.28	6108
8.5	5	1016	7.35	-2.61	1492	1212	10.78	0.83	-1.19	1.94	253

Note: Results aggregate 156 countries. GDP is in trillions of dollars, while population is in billions.

(b) Below-Median Income Countries

Scenario (RCP)	SSP				RFF-SP						
	2100 Base			%	2100 GDP		2100 Pop.		% Impact		
	SSP	GDP	Pop.	Impact	Mean	SD	Mean	SD	Mean	SD	N
2.6	1	354	4.66	-2.81	431	456	8.34	0.75	-2.50	0.47	4309
4.5	2	331	6.44	-3.94	369	395	8.34	0.75	-3.70	0.72	9590
6.0	4	168	7.17	-5.35	398	425	8.34	0.75	-5.57	0.89	6108
8.5	5	576	4.53	-10.20	714	559	8.30	0.77	-9.01	1.60	253

Note: Results aggregate 78 countries. GDP is in trillions of dollars, while population is in billions.

Of the climate scenarios, RCP 8.5 unsurprisingly yields the most negative impacts to world output in the year 2100. Weighting by SSP 5 suggests that global GDP falls by 2.6%, while using RFF-SP projects a decline of 1.2% with standard deviation of 1.9. To compare these results to existing literature, Burke et al. (2015a) focus on the case of RCP 8.5 and SSP 5 to estimate that average global incomes would be reduced by around 23%. The impact is far more negative when we focus on the sample of countries with below-median 2010 incomes, as shown in Table 2b; losses reach 10.2% using SSPs and 9.0% using RFF-SPs. This emphasizes the persistent pattern that poor countries suffer disproportionately from climate change, while rich countries see much smaller damages or in some cases positive impacts.

Beyond aggregate world damages, the heterogeneity in impact is relevant to the level of inequality between countries. To quantify this, Table 3 presents population-weighted Gini coefficients assuming each person in each country earns the country-

level GDP per capita for 2010, using the four RCP scenarios. Under the SSP heading, we use SSP country-level projections to show the Gini coefficient in the absence of climate change in 2100 and the increase in the Gini under each climate scenario. This climate difference is found by subtracting the baseline Gini from the Gini calculated using GDP per capita adjusted by climate impacts. Columns under the RFF-SP header provide means and standard deviations of the baseline Gini and the climate difference for the sample of RFF-SP draws that were linked to each RCP scenario.

Table 3: Population-weighted Gini Coefficients

	SSP			RFF-SP				
			Climate	Base Gini		Climate Impact		
Scenario	SSP	Base Gini	Impact	Mean	SD	Mean	SD	N
Hist.	2010	0.538						
RCP 2.6	SSP 1	0.122	0.016	0.486	0.063	0.013	0.003	4309
RCP 4.5	SSP 2	0.193	0.028	0.485	0.063	0.020	0.004	9590
RCP 6.0	SSP 4	0.527	0.026	0.486	0.063	0.026	0.005	6108
RCP 8.5	SSP 5	0.105	0.065	0.478	0.059	0.041	0.008	253

Note: Results aggregate 156 countries.

2100 Gini coefficients in the absence of climate impacts are lower than the 2010 world Gini in all four RCP scenarios. SSP scenarios in particular have notable, perhaps not credible projected declines in inequality for all scenarios except that linked to RCP 6.0. The climate difference values suggest that climate change increases inequality regardless of the socioeconomic or climate scenario. For example, in RCP 2.6, the Gini coefficient increases by 0.016 using SSPs and an average of 0.013 using RFF-SPs, while under RCP 8.5 the increase is 0.065 using SSPs and an average of 0.041 using RFF-SPs. That climate change increases inequality across all RCPs emphasizes that the impacts are outsized in the most vulnerable populations, even if the average level of damage in the world is modest.

8 Conclusion

This paper quantifies the projected effects of established climate change scenarios on characteristics that affect the carrying capacity of land, which we call location quality. Location quality tends to increase for select countries in currently colder climates and decreases in the tropics and sub-tropics. Using this measure in a model of economic growth, we assess the effects of climate change against a counterfactual

in which location quality is unchanged. Under the most extreme scenario of RCP 8.5, we estimate country-level impacts ranging from -33% to 92%, with a positive correlation between log GDP and climate change impact, so that richer countries on average experience more positive impacts.

We then compare the effects of climate change against the effects of projected population growth, finding that the impact of the latter is consistently the larger of the two. Further, for most countries, uncertainty across climate scenarios implies less uncertainty about economic outcomes than does uncertainty across population scenarios.

Our analysis of climate damages is closely tied to the output of global climate models, and thus shares any limitations that are present in these models. Notably, this means that our analysis may underweight the importance of natural disasters that are likely to become more frequent with global warming.

One of our crucial findings is that climate change will make the natural environment less supportive of human habitation in exactly the places where population growth is already working to raise the burden on that land. The intensification of population pressure disproportionately affects more vulnerable regions, becoming another driver for inequality in economic development.

A notable aspect of our analysis is that we allow for within-country labor mobility in response to climate change, but not for similar mobility between countries. While it is true that climate change will *ceteris paribus* raise the gap in income between rich and poor countries, the income gap between these country groups is already quite large, and migration flows between them are relatively small. Further, while climate change will work to raise the income gap between rich and poor, other economic processes (embodied in the SSP scenarios discussed above) will lower the gap.[25]

A simple reading of our results would say "Don't worry about climate change—the bigger issue is population growth." This is not our interpretation, for several reasons. First, even a finding that population growth is a larger driver of environmental stress than climate change does not in any way lessen the damage being done by that climate change. Second, unlike the effects of population growth, the effects of climate change largely result from decisions and behaviors outside the country that is impacted. More

[25]Conte (2022) estimates that climate-induced international migration within sub-Saharan Africa between 2000 and 2080 will be only 14 million individuals under the current regime of migration barriers. Absent those barriers, this migration would increase to 87 million people.

concretely, in poor countries that will suffer the most from climate change, the vast majority of relevant emissions causing that climate change were and will be the result of economic activity elsewhere in the world. Third, nothing in our analysis addresses the relative costs and unintended consequences of reducing population growth versus mitigating climate change. Finally, the welfare calculus regarding population growth differs markedly from that regarding climate change: having more warming, holding population constant, reduces the average welfare of a fixed set of people. By contrast, reducing population growth, holding climate constant, may raise welfare per capita but lower the number of people who experience that welfare.

References

Acemoglu, Daron, Leopoldo Fergusson, and Simon Johnson (2020) "Population and conflict," *The Review of Economic Studies*, 87 (4), 1565–1604.

Acemoglu, Daron and Simon Johnson (2007) "Disease and development: the effect of life expectancy on economic growth," *Journal of Political Economy*, 115 (6), 925–985.

Arthur, W Brian (1989) "Competing Technologies, Increasing Returns, and Lock-In by Historical Events," *Economic Journal*, 99 (394), 116–131.

Ashraf, Quamrul H, Ashley Lester, and David N Weil (2009) "When does improving health raise GDP?" *NBER Macroeconomics Annual*, 23 (1), 157–204.

Ashraf, Quamrul, David Weil, and Joshua Wilde (2013) "The effect of fertility reduction on economic growth," *Population and Development Review*, 39 (1), 97–130.

Barrage, Lint and William D. Nordhaus (2023) "Policies, Projections, and the Social Cost of Carbon: Results from the DICE-2023 Model," Working Paper 31112, National Bureau of Economic Research.

Black, Duncan and Vernon Henderson (2003) "Urban evolution in the USA," *Journal of Economic Geography*, 3 (4), 343–372.

Burke, Marshall, Solomon M Hsiang, and Edward Miguel (2015a) "Climate and conflict," *Annual Review of Economics*, 7 (1), 577–617.

——— (2015b) "Global non-linear effect of temperature on economic production," *Nature*, 527 (7577), 235–239.

Burzyński, Michał, Christoph Deuster, Frédéric Docquier, and Jaime De Melo (2022) "Climate change, inequality, and human migration," *Journal of the European Economic Association*, 20 (3), 1145–1197.

Carleton, Tamma, Amir Jina, Michael Delgado et al. (2022) "Valuing the global mortality consequences of climate change accounting for adaptation costs and benefits," *Quarterly Journal of Economics*, 137 (4), 2037–2105.

Caselli, Francesco and James Feyrer (2007) "The marginal product of capital," *Quarterly Journal of Economics*, 122 (2), 535–568.

Casey, Gregory, Stephie Fried, and Ethan Goode (2023) "Projecting the Impact of Rising Temperatures: The Role of Macroeconomic Dynamics," *IMF Economic Review*, 71, 688–718.

Casey, Gregory and Oded Galor (2017) "Is faster economic growth compatible with reductions in carbon emissions? The role of diminished population growth," *Environmental Research Letters*, 12 (1), 10–1088.

Chen, Deliang, Maisa Rojas, Bjørn H. Samset et al. (2023) "Framing, Context, and Methods," in *Climate Change 2021 – The Physical Science Basis: Working Group I Contribution to the Sixth Assessment Report of the Intergovernmental Panel on Climate Change*, 147–286: Cambridge University Press.

Ciccone, Antonio and Robert Hall (1996) "Productivity and the Density of Economic Activity," *American Economic Review*, 86 (1), 54–70.

Combes, Pierre-Philippe, Sylvie Démurger, and Shi Li (2017) "Productivity Gains from Agglomeration and Migration in the People's Republic of China between 2002 and 2013," *Asian Development Review*, 34 (2), 184–200.

Combes, Pierre-Philippe and Laurent Gobillon (2015) "The Empirics of Agglomeration Economies," in *Handbook of Urban and Regional Economics*, 5, Chap. 5, 247–348: Elsevier.

Conte, Bruno (2022) "Climate change and migration: the case of Africa," CESifo Working Paper Series 9948, CESifo.

Costinot, Arnaud, Dave Donaldson, and Cory Smith (2016) "Evolving comparative advantage and the impact of climate change in agricultural markets: Evidence from 1.7 million fields around the world," *Journal of Political Economy*, 124 (1), 205–248.

Cruz, Jose-Luis and Esteban Rossi-Hansberg (forthcoming) "The Economic Geography of Global Warming," *Review of Economic Studies*.

Das Gupta, Monica, John Bongaarts, and John Cleland (2011) "Population, poverty, and sustainable development: A review of the evidence," Policy Research Working Paper Series 5719, The World Bank.

Davis, Donald and David Weinstein (2002) "Bones, Bombs, and Break Points: The Geography of Economic Activity," *American Economic Review*, 92 (5), 1269–1289.

Dell, Melissa, Benjamin F Jones, and Benjamin A Olken (2012) "Temperature shocks and economic growth: Evidence from the last half century," *American Economic Journal: Macroeconomics*, 4 (3), 66–95.

Dellink, Rob, Jean Chateau, Elisa Lanzi, and Bertrand Magné (2017) "Long-term economic growth projections in the Shared Socioeconomic Pathways," *Global Environmental Change*, 42, 200–214.

Desmet, Klaus et al. (2021) "Evaluating the Economic Cost of Coastal Flooding," *AmericanEconoimc Journal: Macroeconomics*, 32 (2), 444–486.

Desmet, Klaus and Jordan Rappaport (2017) "The settlement of the United States, 1800–2000: The long transition towards Gibrat's law," *Journal of Urban Economics*, 98 (C), 50–68.

Desmet, Klaus and Esteban Rossi-Hansberg (2015) "On the spatial economic impact of global warming," *Journal of Urban Economics*, 88, 16–37.

Duranton, Gilles (2007) "Urban Evolutions: The Fast, the Slow, and the Still," *The American Economic Review*, 97 (1), 197–221.

Eaton, Jonathan and Zvi Eckstein (1997) "Cities and growth: Theory and evidence from France and Japan," *Regional Science and Urban Economics*, 27 (4), 443–474.

Ehrlich, P (1968) *The Population Bomb*, New York: Sierra Club/Ballantine.

Galor, Oded and Ömer Özak (2016) "The agricultural origins of time preference," *American Economic Review*, 106 (10), 3064–3103.

Hansen, Gary D and Edward C Prescott (2002) "Malthus to Solow," *American Economic Review*, 92 (4), 1205–1217.

Harari, Mariaflavia and Eliana La Ferrara (2018) "Conflict, climate, and cells: a disaggregated analysis," *Review of Economics and Statistics*, 100 (4), 594–608.

Hardin, Garrett (1968) "The tragedy of the commons," *Science*, 162 (3859), 1243–1248.

Henderson, J. Vernon, Dzhamilya Nigmatulina, and Sebastian Kriticos (2021) "Measuring urban economic density," *Journal of Urban Economics*, 125, 103188.

Henderson, J Vernon, Tim Squires, Adam Storeygard, and David Weil (2018) "The global distribution of economic activity: nature, history, and the role of trade," *Quarterly Journal of Economics*, 133 (1), 357–406.

Hsiang, Solomon (2016) "Climate econometrics," *Annual Review of Resource Economics*, 8, 43–75.

Kahn, Matthew E, Kamiar Mohaddes, Ryan NC Ng, M Hashem Pesaran, Mehdi Raissi, and Jui-Chung Yang (2021) "Long-term macroeconomic effects of climate change: A cross-country analysis," *Energy Economics*, 104, 105624.

Kohler, Hans-Peter (2012) "Copenhagen Consensus 2012: Challenge paper on population growth," Working Paper 12-03, Population Studies Center, University of Pennsylvania.

Krugman, Paul (1991) "Increasing Returns and Economic Geography," *Journal of Political Economy*, 99 (3), 483–499.

Krusell, Per and Anthony A Smith, Jr (2022) "Climate change around the world," Working Paper 30338, National Bureau of Economic Research.

Lemoine, Derek (2021) "Estimating the consequences of climate change from variation in weather," Working Paper 25008, National Bureau of Economic Research.

Lustgarten, Abrahm (2020a) "The great climate migration," *New York Times Magazine*, `https://www.nytimes.com/interactive/2020/07/23/magazine/climate-migration.html`.

——— (2020b) "How climate migration will reshape America," *New York Times Magazine*, `https://www.nytimes.com/interactive/2020/09/15/magazine/climate-crisis-migration-america.html`.

——— (2020c) "How Russia wins the climate crisis," *New York Times Magazine*, `https://www.nytimes.com/interactive/2020/12/16/magazine/russia-climate-migration-crisis.html`.

MacManus, K., D. Balk, H. Engin, G. McGranahan, and R. Inman (2021) "Estimating population and urban areas at risk of coastal hazards, 1990–2015: how data choices matter," *Earth System Science Data*, 13 (12), 5747–5801, 10.5194/essd-13-5747-2021.

Malthus, Thomas Robert (1798) *An essay on the principle of population*, London: J. Johnson.

Massetti, Emanuele and Robert Mendelsohn (2018) "Measuring climate adaptation: Methods and evidence," *Review of Environmental Economics and Policy*, 12 (2), 324–341.

McGuirk, Eoin F and Nathan Nunn (forthcoming) "Transhumant pastoralism, climate change, and conflict in Africa," *Review of Economic Studies*.

Michaels, Guy, Ferdinand Rauch, and Stephen Redding (2012) "Urbanization and Structural Transformation," *Quarterly Journal of Economics*, 127 (2), 535–586.

Millar, R. J., Z. R. Nicholls, P. Friedlingstein, and M. R. Allen (2017) "A modified impulse-response representation of the global near-surface air temperature and atmospheric concentration response to carbon dioxide emissions," *Atmospheric Chemistry and Physics*, 17 (11), 7213–7228, 10.5194/acp-17-7213-2017.

Newell, Richard G., Brian C. Prest, and Steven E. Sexton (2021) "The GDP-Temperature relationship: Implications for climate change damages," *Journal of Environmental Economics and Management*, 108, 102445.

Newman, R. and I. Noy (2021) "The global costs of extreme weather that are attributable to climate change," *Nature Communications*, 14 (6103), 1–13.

Nordhaus, William D (2006) "Geography and macroeconomics: New data and new findings," *Proceedings of the National Academy of Sciences*, 103 (10), 3510–3517.

O'Neill, Brian C., Elmar Kriegler, Keywan Riahi, Kristie L. Ebi, Stephane Hallegatte, Timothy R. Carter, Ritu Mathur, and Detlef P. Van Vuuren (2014) "A new scenario framework for climate change re- search: the concept of shared socioeconomic pathways," *Climatic Change*, 122 (3), 387–400.

Piontek, Franziska, Laurent Drouet, Johannes Emmerling et al. (2021) "Integrated perspective on translating biophysical to economic impacts of climate change," *Nature Climate Change*, 11 (7), 563–572.

Rennert, Kevin, Frank Errickson, Brian C. Prest et al. (2022) "Comprehensive Evidence Implies a Higher Social Cost of CO_2," *Nature*, 610, 687—-692.

Rennert, Kevin, Brian C. Prest, William A. Pizer et al. (2021) "The Social Cost of Carbon: Advances in Long-term Probabilistic Projections of Population, GDP, Emissions, and Discount Rates.," *Brookings Paper on Economic Activity*, 223–275.

Riahi, Keywan, Detlef P. van Vuuren, Elmar Kriegler et al. (2017) "The Shared Socioeconomic Pathways and their energy, land use, and greenhouse gas emissions implications: An overview," *Global Environmental Change*, 42, 153–168.

Rigaud, Kanta Kumari, Alex de Sherbinin, Bryan Jones et al. (2018) "Groundswell: Preparing for Internal Climate Migration,"Technical report, World Bank, Washington, DC.

Rosenthal, Stuart and William Strange (2004) "Evidence on the nature and sources of agglomeration economies," in Henderson, J. V. and J. F. Thisse eds. *Handbook of Regional and Urban Economics*, 4, Chap. 49, 2119–2171: Elsevier.

Samir, KC and Wolfgang Lutz (2017) "The human core of the shared socioeconomic pathways: Population scenarios by age, sex and level of education for all countries to 2100," *Global Environmental Change*, 42, 181–192.

Santos Silva, J. M. C. and Silvana Tenreyro (2006) "The Log of Gravity," *The Review of Economics and Statistics*, 88 (4), 641–658.

Stocker, Thomas F, Dahe Qin, G-K Plattner et al. (2013) "Summary for Policymakers," in *Climate change 2013: the physical science basis. Contribution of Working Group I to the Fifth Assessment Report of the Intergovernmental Panel on Climate Change*, 33–115: Cambridge University Press.

Tol, Richard SJ (2012) *Climate Economics: Economic Analysis of Climate, Climate Change and Climate Policy*: Edward Elgar.

——— (2021) "The economic impact of weather and climate,"Technical Report 8946, Center for Economic Studies and Ifo Institute for Economic Research, Munich.

United Nations, Department of Economic and Social Affairs, Population Division (2019) *World Population Prospects 2019, Volume I: Comprehensive Tables (ST/ESA/SER.A/426)*, New York: United Nations.

Vörösmarty, Charles J, Pamela Green, Joseph Salisbury, and Richard B Lammers (2000) "Global water resources: vulnerability from climate change and population growth," *Science*, 289 (5477), 284–288.

Welch, Ivo (2024) "The IPCC Shared Socioeconomic Pathways (SSPs): Explained, Critiqued, Replaced."

White House (2021) "Report on the impact of climate change on migration,"Technical report, The White House, Washington, DC, USA.

Young, Alwyn (2005) "The Gift of the Dying: The Tragedy of AIDS and the Welfare of Future African Generations," *Quarterly Journal of Economics*, 120 (2), 423–466.

Online Appendices

A Methodology

This appendix discusses the data and methodology in greater detail. As introduced in Section 3, the specification for our Poisson regression is:

$$E(L_{i,c}/Z_{i,c} \mid C_c, x_{i,c}) = exp(C_c + x_{i,c}\beta) \tag{A1}$$

where C_c is a country fixed effect and $x_{i,c}$ the vector of characteristics for grid cell i in country c. Our dependent variable is grid-cell population density from 2010, for which our preferred source is the European Union's Global Human Settlements population layer (GHS-POP). $x_{i,c}$ is a set of 54 characteristics for which both 2010 data and 2100 projections are available: 8 strictly geographic characteristics that do not change, 33 agro-climatic variables and 11 crop suitability indices taken directly from the U.N. Food and Agricultural Organization's Global Agro Ecological Zones v4 dataset, and two variables described below: maximum potential caloric yield and temperature variability.[1]

Elevation, latitude, ruggedness, distance to the coast, and a set of four dummies indicating the presence of a coast, a navigable river, a major lake, and a natural harbor within 25 km of a cell centroid from Henderson et al. (2018) comprise the set of 8 time-invariant geographic variables. The 33 GAEZ variables used represent the majority of continuous variables from its Theme 2: Agro-climatic resources. We exclude variables that overlap in definition, are linearly dependent, assume irrigation, indicate beginning dates, are missing data for a significant area of the world, or have a value of 0 for more than 95 percent of observations. The variables that are dropped under these conditions are: annual temperature amplitude, quarterly P/PET ratios, net primary production with irrigation, beginning date of the longest component length of growing period, beginning date of the earliest growing period, reference evapotranspiration deficit, snow stock at calendar year end, soil moisture condition at calendar year end, and number of days with a maximum temperature of 45 degrees Celsius. We further exclude the number of consecutive days with average precipitation over 45 mm and the average annual sum of precipitation on such days; variation in these two measures is overwhelmingly concentrated in small regions of developing

[1]This dataset can be accessed at `https://gaez.fao.org/`.

countries.

To this we add crop suitability indices for banana, cassava, maize, sweet and white potato, dryland and wetland rice, soybean, sorghum, wheat, and yam, which are the largest crops in terms of worldwide calorie production. Because crop suitability index projections are only generated assuming "high input," or commercialized agriculture, we use "high input" crop suitability indices for both the historical and future period for consistency.

We further include in our baseline regression a composite variable indicating the maximum potential caloric yield across these 11 crops. Following Galor and Özak (2016), potential caloric yields in kilograms (dry weight) per hectare per year for each crop are taken from GAEZ and converted into kilo-calories per hectare using caloric content values provided by the United States Department of Agriculture Nutrient Database for Standard Reference. The maximum across the 11 crops is then calculated for each grid cell.

Finally, we construct a variable to capture temperature variability in each period. Using daily average surface temperature values, we calculate the standard deviation of the linearly detrended daily average temperature over a 30-year period for each day in the calendar year. We then take the average of these 365 standard deviation values. This mimics measures of volatility used in environmental science papers such as Chan et al. (2020) while avoiding concerns about the difference in seasons between the northern and southern hemispheres. Other aspects of volatility are captured by variables in GAEZ: the number of days above 30, 35 and 40 degrees and below 15, 10 and 0 degrees; Annual temperature amplitude; Longest period of consecutive dry days in temperature growing period; Number of consecutive days with average precipitation over 30 mm; and maximum sum of precipitation on consecutive days when average daily precipitation is over 30 mm.

Complete daily average surface temperature data are not available for all grid cells from 1981 to 2010. Instead, we use daily temperature values generated by climate models to calculate year-to-year variability of daily temperature.[2] Specifically, for each of the five climate models included in GAEZ we calculate grid-cell averages of year-to-year volatility by day. We then take the mean of this value across the ensemble

[2]The "2010" value was generated using 1981–2005 temperatures from each climate model's historical experiment; projected 2071–2100 temperatures were used for the 2100 value for each climate scenario.

of five models.

Table A1 reports the resulting estimates for equation (A1).

Table A1: Grid Square Regression Coefficients

	Coefficient	S.E.
Abs(Latitude)	0.032***	(3.89e-03)
Elevation (m)	−1.77e-04***	(4.26e-05)
Distance to coast (000 km)	−6.82e-07***	(3.44e-08)
Coast dummy	0.388***	(0.029)
Harbor dummy	0.822***	(0.024)
Navigable river dummy	0.749***	(0.029)
Ruggedness (000s)	−1.87e-06***	(1.24e-07)
Lake dummy	0.716***	(0.147)
Adjusted LGP for evaluating agro-climatic constraints	5.84e-03***	(5.62e-04)
Length of longest component LGP	2.32e-03***	(3.98e-04)
Longest consecutive dry days in LGPt=5	−7.3e-04*	(3.92e-04)
Number of dry days during LGPt=5	−7.65e-03***	(1.49e-03)
Total number of growing period days	5.33e-03***	(1.36e-03)
Total number of LGP days in component LGPs > 20 days	−7.69e-03***	(1.1e-03)
Net primary production (rain-fed)	−4.53e-05***	(3.02e-06)
Annual P/PET ratio (*100)	2.89e-03	(2.73e-03)
P/PET (*100) for days with mean temperature > 5 deg. C	−0.02***	(2.18e-03)
Seasonal P/PET ratio (*100) in summer	−2.05e-03***	(6.27e-04)
Seasonal P/PET ratio (*100) in winter	−1.05e-03***	(3.81e-04)
Number of consecutive days with average precipitation > 30 mm	0.143	(0.123)
Total number of rain days (days with precipitation > 1 mm)	−6.59e-03***	(1.4e-03)
Modified Fournier Index (mm)	2.84e-04***	(3.72e-05)
Annual precipitation (mm)	2.51e-04*	(1.35e-04)
Mean max. sum of precip. on consec. > 30 mm av. precip. days	−4.53e-03	(4.09e-03)
Reference actual evapotranspiration (using AWC=100 mm/m)	1.03e-03***	(1.85e-04)
Reference potential evapotranspiration (using AWC=100 mm/m)	−1.89e-03***	(1.09e-04)
Number of days with max temperature > 35 deg. C	−1.23e-03***	(4.27e-04)
Number of days with max temperature > 40 deg. C	4.07e-03***	(7.72e-04)
Number of days with min temperature < 0 deg. C	−1.13e-03	(8.3e-04)
Number of days with min temperature < 10 deg. C	−9.73e-04**	(3.97e-04)
Number of days with min temperature < 15 deg. C	2.27e-03***	(3.47e-04)
Number of days with mean temperature > 10 deg. C (LGPt=10)	−5e-03*	(2.79e-03)
Number of days with mean temperature > 5 deg. C (LGPt=5)	0.019***	(3.15e-03)
Annual temperature amplitude (deg. C)	−0.037***	(0.013)
Mean annual temperature (deg. C)	0.522***	(0.035)

Snow-adjusted cold temperature limit	7.34e-04***	(2.15e-04)
Temperature of coolest month (deg. C*100)	−1.52e-03***	(2.97e-04)
Annual temperature sum for days with mean temp. > 10 deg. C	1.54e-03***	(3.75e-04)
Annual temperature sum for days with mean temp. > 5 deg. C	−2.81e-03***	(3.83e-04)
Air frost number	−0.68	(2.391)
Snow-adjusted air frost number	1.095	(2.507)
Maize suitability index	−5.78e-05***	(1e-05)
Dryland rice suitability index	6.65e-06	(5.93e-06)
Wetland rice suitability index	−1.83e-06	(6.3e-06)
Wheat suitability index	7.78e-06	(8.41e-06)
Cassava suitability index	−2.82e-05***	(1.01e-05)
Soybean suitability index	9.01e-05***	(8.75e-06)
White potato suitability index	4.03e-05***	(9.68e-06)
Sorghum suitability index	6.58e-05***	(7.99e-06)
Sweet potato suitability index	5.15e-05***	(8.46e-06)
Yam suitability index	−9.28e-05***	(9.73e-06)
Banana suitability index	2.26e-05***	(8.4e-06)
Year-to-year volatility of daily temperature	−0.32***	(0.031)
Max. potential caloric yield (kcal/ha)	−1.9e-09	(2.1e-09)
R^2_{dev}		0.568
Observations		237023

Note: LGP is the length of the growing period; LGPt=n is the temperature growing period, which provides the number of days with mean temperature over n degrees Celsius. P/PET is the ratio of precipitation to potential evapotranspiration. All crop suitability indices are based on the following assumptions: high inputs, rain-fed, CO2 fertilization. *p<0.1; **p<0.05; ***p<0.01

Estimating $\hat{\beta}$ with 1980–2010 data allows us to generate location quality for any period when $x_{i,c}$ is available. We first generate location quality for 2010 using $x_{i,c,2010}$. Future location quality can be predicted given projected values of $x_{i,c,2100}$. GAEZ provides projections to the year 2100 for four climate scenarios[3] for each of the five included global climate models; we predict 2100 location quality for each climate model and climate scenario. Given the ensemble of results, we take the geometric mean of land quality as our preferred land quality values.[4]

[3]RCPs 2.6, 4.5, 6.0, and 8.5. RCPs refer to Representative Concentration Pathways, which were adopted in IPCC Assessment Report 5.

[4]Multi-model ensemble means tend to improve accuracy (Frankcombe et al., 2018) and are used to generate headline predictions of climate change for IPCC assessment reports.

B Comparison of Population Datasets and Cell-Level Specifications

In this appendix we first compare the distribution of population density in our main population data source, GHS-POP, to two alternatives, GPWv4 and LandScan. We then compare regression results using our baseline Poisson specification and a log-linear alternative, using all three datasets—a total of six variants. Specifically, we compare goodness of fit and fitted values in a regression of population on geographic characteristics. All three global datasets report population counts for 30-arc-second by 30 arc-second pixels in Plate Carrée (latitude/longitude) projection. The area of a pixel is 0.86 square km at the equator, decreasing with the cosine of latitude.

The Gridded Population of the World version 4 (GPWv4; CIESIN 2017) is the simplest of the three. The underlying data are population estimates for administrative regions (polygons) from censuses circa 2010. When there is no census in exactly 2010, values are extrapolated or interpolated from multiple censuses. Population is assumed to be distributed evenly within an administrative region. GPWv4's effective spatial resolution thus depends on what information individual countries provide, with richer countries typically providing data for finer regions, down to enumeration units, or even block level data. There is substantial variation within countries as well, with higher resolution in more densely populated regions. Of 12.9 million input polygons worldwide, only 2.4 million are from outside the United States. A grid cell crossing a polygon boundary is assigned a population density that is the areally-weighted average of its constituent polygons.

The European Union's Global Human Settlements population layer (GHS-POP; Schiavina et al., 2019; Carneiro Freire et al., 2016) reallocates GPWv4 estimates within administrative polygons based on a companion dataset, GHS-BUILT (Corbane et al., 2018, 2019) that defines built-up pixels as seen in Landsat 30-meter resolution satellite data circa 2015. In the rare cases where there is no built-up area visible in a region, it reverts to the GPWv4 estimates. Its land area measures are taken directly from GPWv4. More information about GHS can be found in Florczyk et al. (2019).

LandScan uses a proprietary algorithm to provide population estimates based on a much wider set of inputs that include census population data and satellite imagery at higher resolution than Landsat. While the algorithm is not publicly documented and changes from year to year, in the recent past input data have also included

information on elevation, slope, and land cover, as well as locations of road and rail networks, hydrologic features and drainage systems, utility networks, airports, and populated urban places. LandScan reports estimates of ambient population averaged throughout the day, whereas the other two datasets report nighttime (residential) population estimates. A recent explanation of LandScan for an academic audience can be found in Rose and Bright (2014).

We rely on GHS-POP as our primary source, and consider GPWv4 and LandScan for robustness here. GHS-POP's use of building cover to redistribute people within census units is very likely to provide more accuracy than GPWv4's assumption of uniform density within large administrative units.

LandScan aims to achieve the same goal of redistributing population based on built cover. However, as noted, it uses other information in making assessments, including higher resolution satellite imagery. LandScan may thus do a better job of finding the built environment in rural locations and it may have greater accuracy in dense but low income cities with coarse population data.

However LandScan has four main drawbacks. First, it has historically used coarse census data as a benchmark outside of the United States.[5] While better satellite imagery can better define the built environment, to convert that to population one still needs fine-grained census population data. Second and more importantly, LandScan's algorithm uses physical features like elevation directly to predict population density. This raises the possibility that our regressions will end up simply predicting LandScan's algorithm rather than true population density. Third, LandScan's algorithm changes from year to year and is not documented. Finally LandScan measures the ambient population over the 24 hours of a day, making inferences about where people work and for how many hours of the day, without, as we understand it, much if any spatial economic census data which are unavailable for many developing countries anyway. This seems likely to add error without benefit for our purposes.

Figure B1 Panel A reports the cumulative distribution function (CDF) of log population density according to the three datasets, with zeros in each dataset replaced with that dataset's minimum nonzero value before logging. The figure shows that the three data sets treat grid squares with tiny densities very differently. For example,

[5]LandScan has not released details about its current census data, but as of its 2009 version: "Outside the USA LandScan used 79,590 administrative units for ambient modeling. By contrast, GPWv3 uses 338,863 units outside of the US." Source: `https://sedac.uservoice.com/knowledgebase/articles/41665-what-are-the-differences-between-gpw-grump-and-la`

Figure B1: Population Distributions by Grid Square Worldwide

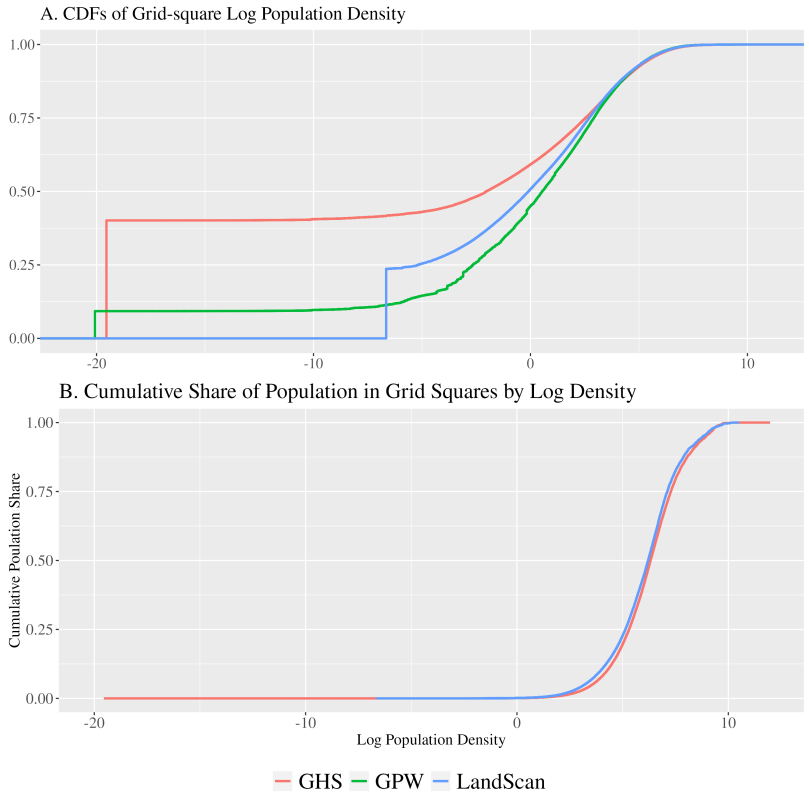

in GHS-POP about 40% of cells have no people, with nonzero densities starting at $0.0000000033/km^2$, while in LandScan only about 24% of grid squares are zeroes, with non-zero densities starting at about $0.0013/km^2$. By population densities of about $50/km^2$ ($exp(3.9)$), the three lines converge, at which point about 85% of pixels have been accounted for. Panel B of Figure B1 analogously reports cumulative population by density. It shows that less than 10% of the world population lives at a density under $50/km^2$. However, since our unit of analysis is the grid square, these tiny densities potentially play an important role.

In implementing the log-linear specification, we converted zeroes in each dataset to the smallest non-zero value in that dataset before logging. We also tried assigning the minimum nonzero value in LandScan to zeroes in all three datasets datasets before logging. As shown in Figure B1, LandScan has by far the largest minimum non-zero density of the three datasets.

Figure B2 compares cell-level predicted values across the three datasets. Using the Poisson specification (Equation (4)), the first column of plots shows that all three

Figure B2: Predicted Values

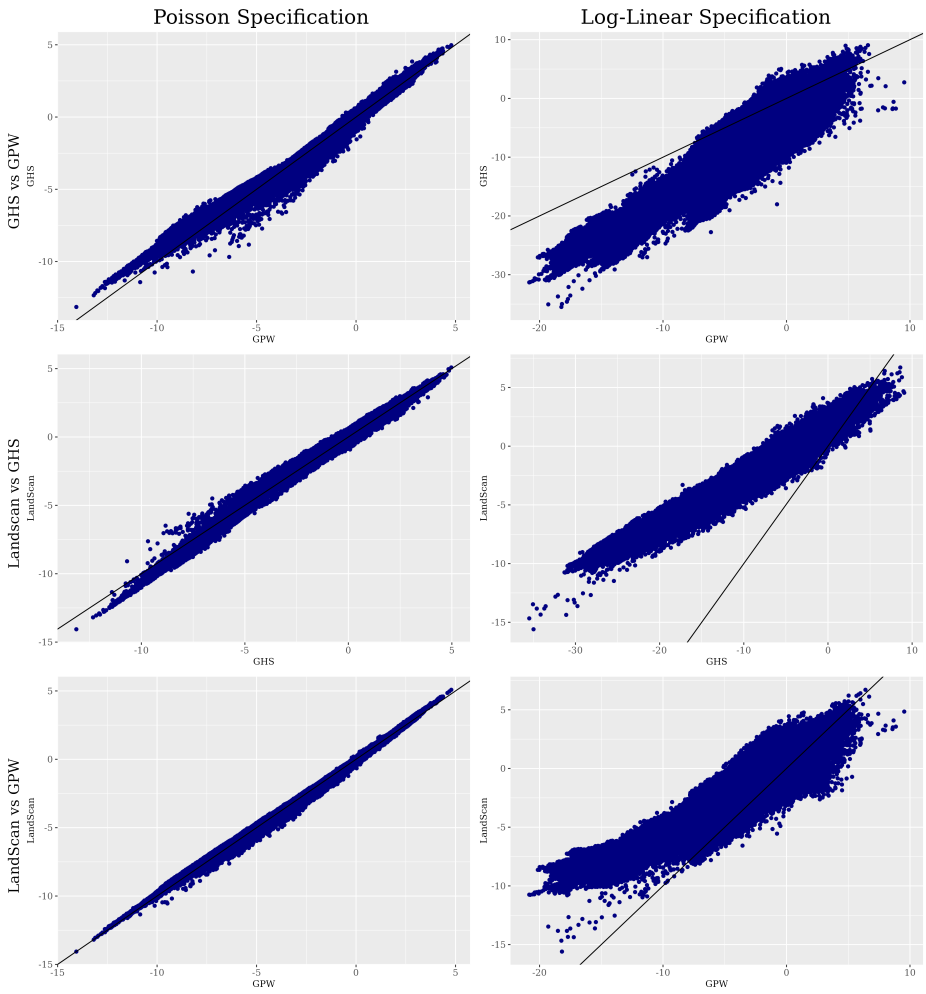

data sets give very similar predicted values. This is because the Poisson specification makes little distinction between cells that have moderately low density and those that have extremely low density. By contrast, in the second column, there are large differences across datasets when using the log-linear specification, driven by the differing treatments of low density regions.

Table B2 reports goodness of fit measures for the log linear and Poisson specifications. In the first 3 rows zeros are assigned their dataset-specific minimum non-zero value. In rows 4 and 5 zeros in GHS-POP and GPWv4 are assigned the LandScan minimum value.

Figure B3 compares country-level impacts of climate change as a percentage of the baseline GDP using log-linear and Poisson specifications. Poisson values are

Table B2: Goodness of Fit for Grid Cell Level Regressions

	Log-linear	Poisson
GHS	0.597	0.568
GPW	0.757	0.621
LandScan	0.738	0.594
GHS Censored	0.660	0.568
GPW Censored	0.800	0.621

Note: 156 countries. R^2 values for log-linear and R^2_{DEV} for Poisson regressions

identical to those in Figure 5. Here, impacts for countries that see large losses, and especially gains, in 2100 are exaggerated in the log-linear specification relative to the Poisson. In an extreme case, Finland is projected to see 92% higher GDP from climate change in the Poisson specification but 1095% higher in the log-linear specification. These larger magnitudes of positive impacts in the log-linear specification imply that climate change will lead to an overall increase in world GDP of 30.0% under SSP5, in comparison to the projected decline of 2.6% using the Poisson model.

Figure B3: Country-Level Impacts

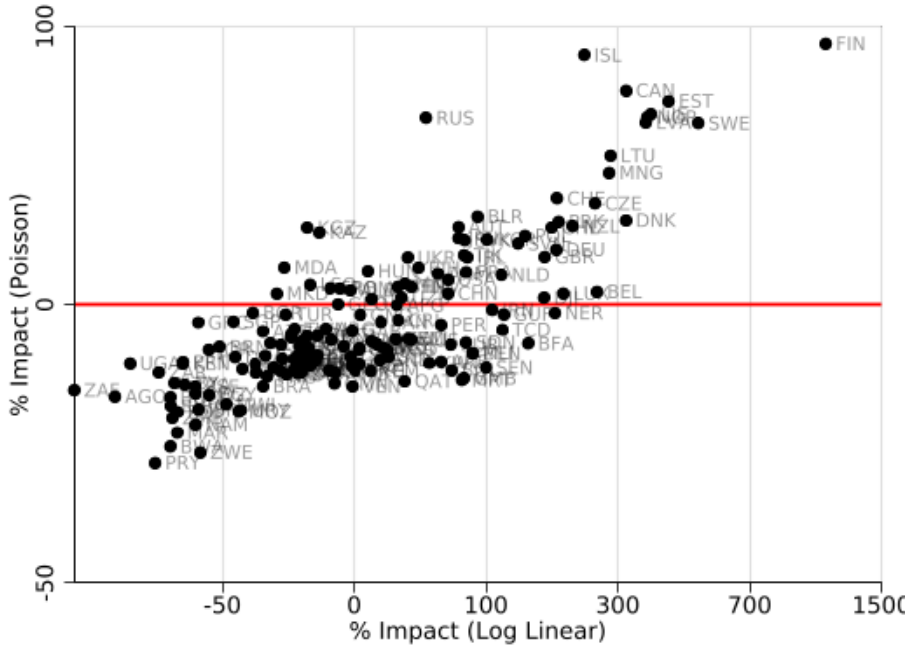

C Variation Across Climate Models

Our main results rely on the ensemble mean of five climate model forecasts. Here we discuss the variation in projections across these forecasts. Appendix Figure C1 shows the grid-level standard deviation of our projected location quality measure across the five climate models.

Calculating the grid-level standard deviation of our projected location quality measure across the five climate models shows that the largest variation among models tends to be in the northern part of the Northern hemisphere as well as the Sahara Desert, although there are other, more localized areas of disagreement in specific climate scenarios. Specifically, we see high variation in the Western Ghats for RCP 6.0 and in Minas Gerais in Brazil for RCP 8.5. Both of these are driven by unusually negative values from a single model (MIROC).

For each climate model we also calculate country-level projected changes in average location quality (ALQ) over the period 2010–2100 under the RCP 8.5 scenario. These are presented in Appendix Figure C2. Panel (a) uses area-weighted ALQ, while (b) uses population-weighted ALQ. The two panels are similar. In general, these country-level projections are highly correlated across the different climate models and each is well correlated with the ensemble mean. However, there are notably larger cross-models differences in projections for countries that are expected to have improved average location quality (upper right of each graph). These tend to be rich countries. Among countries where location quality is expected to decline, there is more accord among the models.

While within-model uncertainty—either from parameters or initial conditions—must also be acknowledged for each climate model, we are not equipped to address this additional source of uncertainty.[6]

[6]The IPCC Assessment Report 4 discusses these issues and the degree of uncertainty they impart in section 10.5.

Figure C1: Grid-Cell Variations in Location Quality Across Climate Models

(a) RCP 2.6

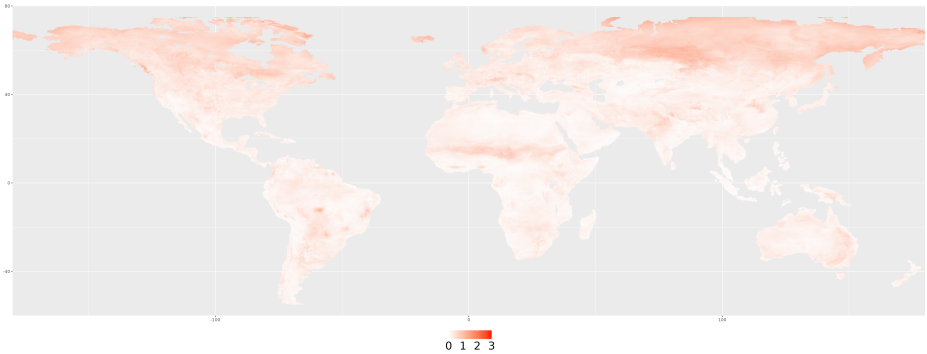

(b) RCP 4.5

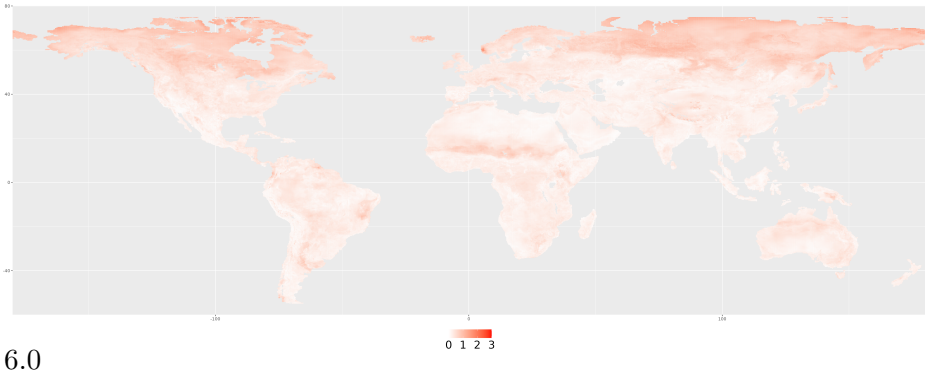

(c) RCP 6.0

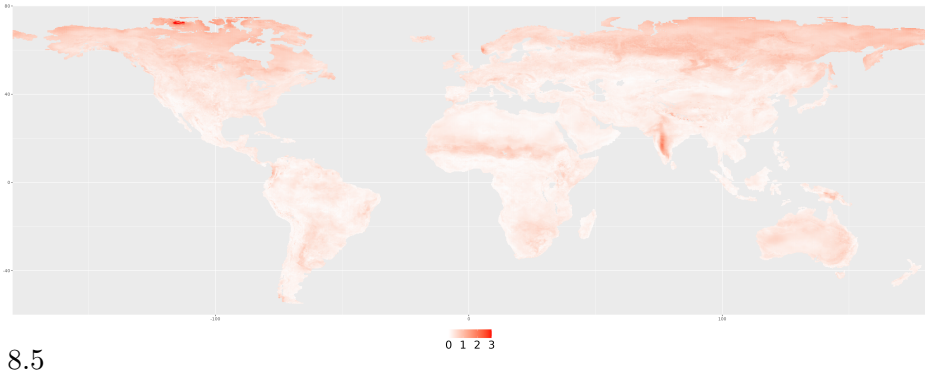

(d) RCP 8.5

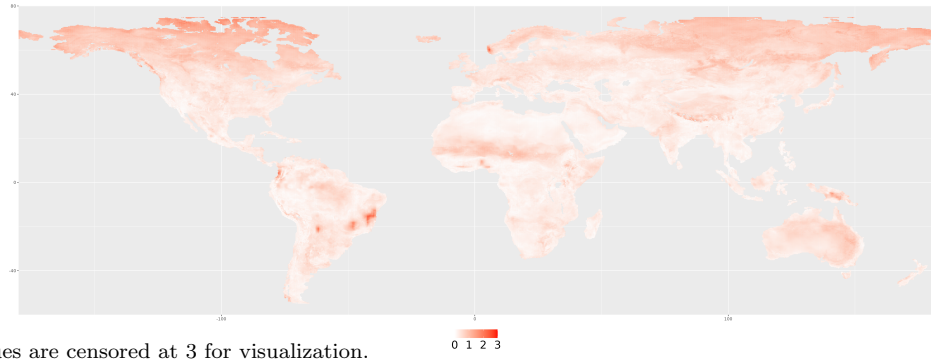

Note: Values are censored at 3 for visualization.

Figure C2: Comparison of Country-level changes to *ALQ* by Climate Model

(a) Area-weighted *ALQ* (b) 2010 Population-weighted *ALQ*

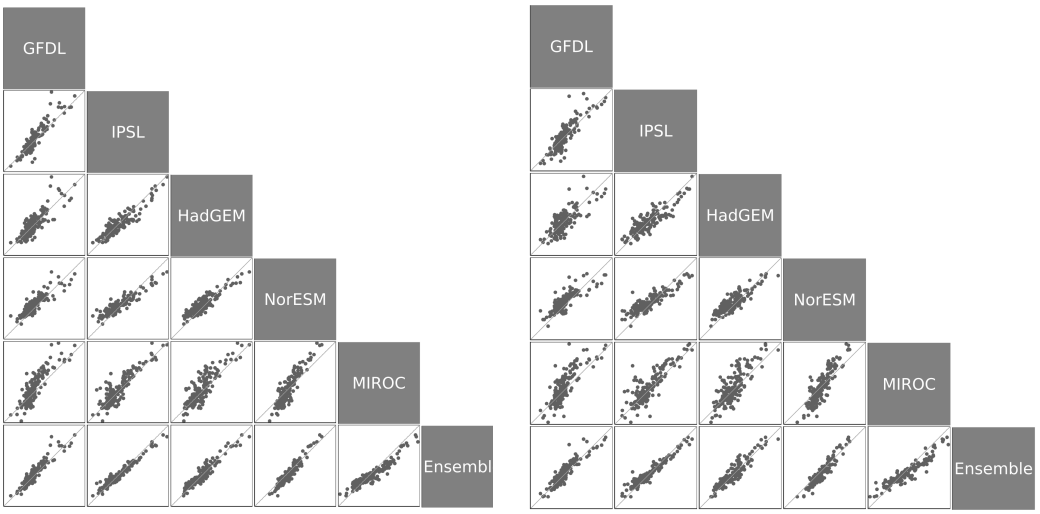

Note: Each cell depicts a scatterplot comparing the log difference in *ALQ* from 2010 to 2100 projected by two different models. The range of each axis is -1.86–2.13 (a) and -1.86–2.63 (b). The diagonal line represents model agreement.

D Robustness to Choice of Sample Countries

One concern regarding our grid-cell regression is that the land characteristics included in our regression may impact economic outcomes differently depending on a country's stage of development. Correspondingly, the effect of a change in a particular characteristic may have a different effect in poor vs. rich countries. For example, a reduction in rainfall in an already dry climate could be devastating in a region reliant on smallholder agriculture, but would have a marginal effect in a richer region that imports its food from elsewhere. As a robustness check, we thus re-estimate our grid-cell level Poisson regressions for measuring location quality by interacting variables included in the baseline regression with an indicator of whether the grid cell's country GDP was above or below the median in 2010. In this way, we allow the set of rich and poor countries to have different coefficients for each included variable. These two sets of estimated coefficients are used to form projections of the change in location quality due to climate change for the sample of all countries with below-median GDP per capita. We focus on poor countries because the analysis in the main text shows that it is generally in these countries that climate change is expected to have the most

negative effects.

A priori it is not clear whether coefficients estimated on today's rich or today's poor countries would be more appropriate for predicting the effect of climate change in the year 2100 on today's poor countries. Poor countries are more reliant on agriculture than are rich ones, but as noted by Henderson et al. (2018), geographic variables that measure suitability for agriculture are less predictive of the distribution of population for poor countries than they are for rich countries. Further, under some of the Shared Socioeconomic Pathways described in Section 7, most of today's poor countries will have reached levels of development comparable to those of today's upper-middle income countries by 2100. At the same time, today's poor countries might have permanent unobserved characteristics that will persist to the year 2100.

Figure D1 shows projected country-level impacts from climate change over the period 2010–2100 under RCP 8.5, comparing baseline coefficients (horizontal axis) and alternate coefficients (vertical axis) for the sample of below-median income countries. Overall, the figure shows that the predicted effects of climate change are fairly similar. Looking first at panel D1a, only 5 countries that are projected to have negative impacts using the baseline estimates see positive impacts using the below-median sample estimates, and 3 countries see the opposite switch. In panel D1b, 4 countries with negative impacts using the baseline estimates see positive impacts using the above-median sample coefficients and 2 countries see the opposite switch. The correspondence between the two projections is fairly tight for the majority of countries that will experience deterioration, but more scattered among those where location quality will improve.

Finally, Table D1 (corresponding to the first panel of Table 2 in the main text) aggregates these country-level impacts for the below-median sample under various climate scenarios and socioeconomic projections. We see that the baseline estimate yields greater damages than either the below-median or the above-median estimates, and that the above-median estimates in turn yield greater damages than the below-median estimates. While these results are a bit puzzling, they certainly give no reason to think that in using the baseline estimates for the world as a whole, rather than projecting poor-country damages using estimates from poor countries alone, we are understating the impact of climate change.

Figure D1: Comparisons of Country-Level Impacts from Climate Change

(a) Below-Median GDP Coefficients

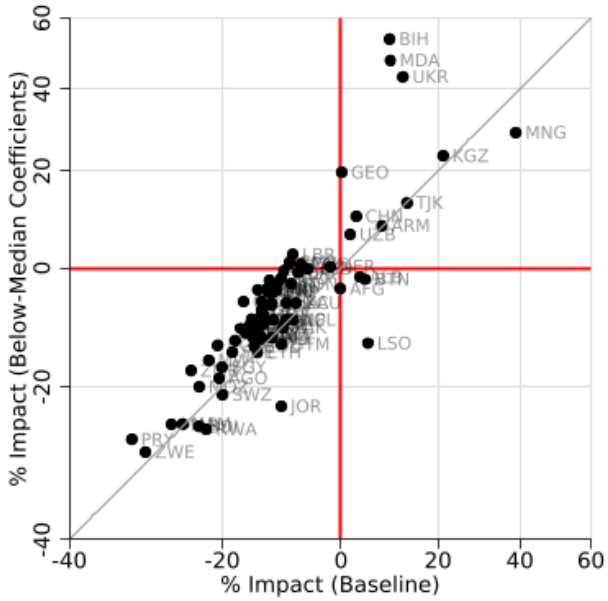

(b) Above-Median GDP Coefficients

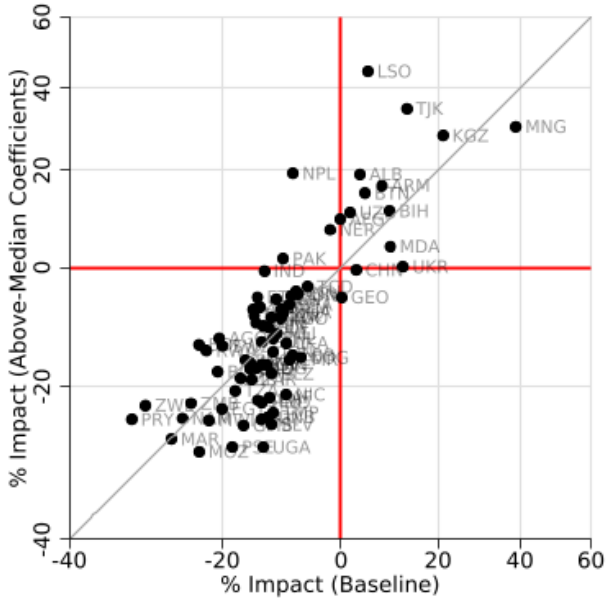

Note: Figure plots the percentage impact of climate change in 2100 using RCP 8.5 and the U.N. medium variant population projection under perfect mobility assumptions for the 78 countries with below-median 2010 GDP on both axes. Horizontal axis estimates use baseline coefficients, while vertical axis estimates use coefficient fitted for below-median countries in panel (a) and coefficients fitted for above-median countries in panel (b).

Table D1: 2100 Impacts as Percentage of Aggregate GDP

	SSP		RFF-SP % Impact		
Scenario	SSP	% Impact	Mean	SD	N
A. % Impact: Baseline Coefficients					
RCP 2.6	SSP 1	-2.81	-2.50	0.47	4309
RCP 4.5	SSP 2	-3.93	-3.70	0.72	9590
RCP 6.0	SSP 4	-5.36	-5.57	0.89	6108
RCP 8.5	SSP 5	-10.22	-9.01	1.60	253
B. % Impact: Below-Median Coefficients					
RCP 2.6	SSP 1	-2.35	-1.70	0.77	4309
RCP 4.5	SSP 2	-2.38	-1.85	1.04	9590
RCP 6.0	SSP 4	-2.45	-2.70	1.34	6108
RCP 8.5	SSP 5	-4.92	-3.60	1.86	253
C. % Impact: Above-Median Coefficients					
RCP 2.6	SSP 1	0.26	-0.10	0.46	4309
RCP 4.5	SSP 2	0.31	-0.60	0.73	9590
RCP 6.0	SSP 4	-2.70	-3.49	0.71	6108
RCP 8.5	SSP 5	-6.73	-6.86	1.47	253

Note: This table is an aggregation of 78 countries. GDP is in trillions of dollars, while population is in billions.

E Average Location Quality by Region

The first column of Table E1, Panel (a) reports ALQ for the world and by continent, where Europe includes all of Russia. As in the main text, world average location quality for 2010 is normalized to one by construction from equation (5). In the remaining columns of Table E1, Panel (a), we repeat this exercise for 2100 under the four different RCP emissions scenarios, keeping the weights in Equation (5) and changing the characteristics x according to each RCP scenario. The second panel of Table E1 repeats the exercise using population rather than area weights.

Table E1: World *ALQ* Change

(a) Area-weighted *ALQ*

Continent	Historical	RCP 2.6	RCP 4.5	RCP 6.0	RCP 8.5
World	1.000	1.033	1.068	1.078	1.102
Africa	0.738	0.645	0.574	0.538	0.410
Americas	1.101	1.055	1.078	1.069	1.097
Asia	0.772	0.758	0.742	0.724	0.696
Europe	1.316	1.770	2.051	2.189	2.538
Oceania	1.484	1.401	1.413	1.444	1.335

(b) 2010 Population-weighted *ALQ*

Continent	Historical	RCP 2.6	RCP 4.5	RCP 6.0	RCP 8.5
World	3.111	2.980	2.948	2.923	2.780
Africa	1.721	1.464	1.292	1.204	0.916
Americas	3.666	3.335	3.404	3.328	3.127
Asia	2.663	2.430	2.329	2.264	2.086
Europe	6.578	7.633	8.068	8.400	8.909
Oceania	18.148	15.847	16.661	17.678	15.051

F Robustness of Location Quality to Variable Choice

This appendix conducts robustness checks for an assortment of variant specifications. For each alternate specification, we provide appendix figures that map the log difference in location quality from 2010 to 2100 under RCP 8.5 and plot the change in *ALQ* from 2010 to 2100 under RCP 8.5 using this alternate specification against that using the baseline specification. A table of world-level climate impacts is also shown.

F.1 Quadratic of Temperature and Precipitation

In this specification, we limit our set of regressors to the quadratic of mean annual temperature and precipitation, as well as the country fixed effects that are present in all the specifications that we examine.

Figure F1: Quadratic of Temperature and Precipitation

(a) Log Difference of Location Quality

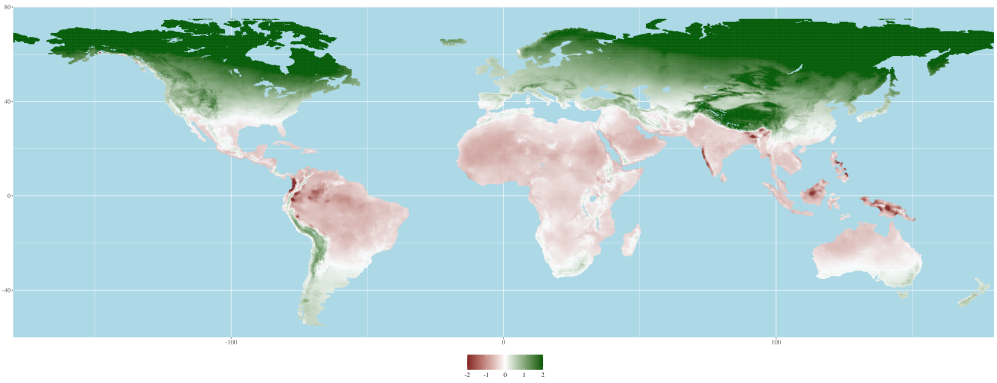

(b) Country-Level Log Difference in *ALQ*

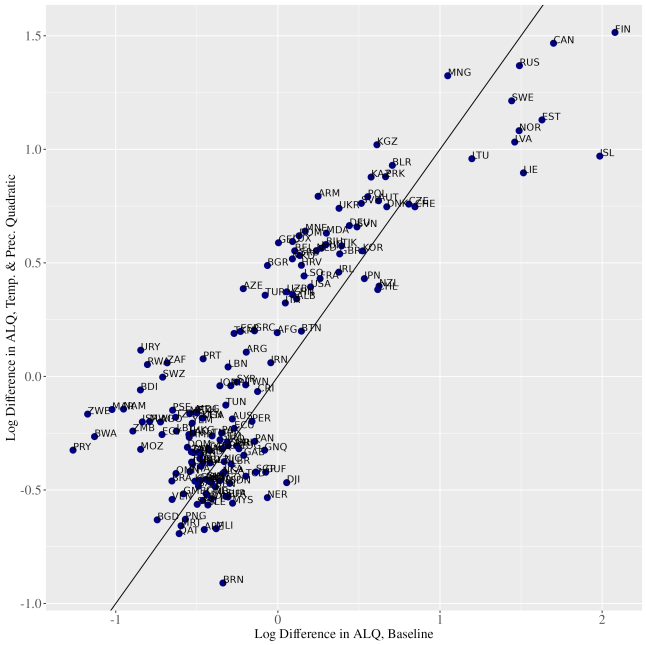

As the figure shows, using the richer set of covariates from our baseline specification paints a significantly different picture than the restricted set. Particularly among poor countries, there are many where the decline in land quality is more than 50 log points greater in the baseline specification than in the restricted version. Comparing the table here with the corresponding Table 2 in the main text: world GDP *rises* under all of the climate scenarios using the restricted specification, while it falls under all of them using our baseline; focusing on countries with year 2010 income below the

Table F1: 2100 Impacts as Percentage of Aggregate GDP

Sample	Full			Below Median Income		
	SSP	RFF-SP Impact		SSP	RFF-SP Impact	
Scenario	Impact	Mean	SD	Impact	Mean	SD
RCP 2.6	1.33	2.41	0.59	−0.62	−0.23	0.60
RCP 4.5	1.31	3.04	1.01	−1.95	−1.38	1.12
RCP 6.0	3.42	3.38	1.17	−0.99	−1.73	1.26
RCP 8.5	1.54	3.35	1.96	−6.25	−4.28	2.13

Note: Results aggregate 156 countries in the full sample and 78 countries in the below median income countries sample. Impacts are in percentages.

median, the negative impact of climate change in the most extreme scenario (RCP 8.5) is twice as large using our baseline specification as in the restricted case.

F.2 GAEZ variables only

In this specification, we restrict our set of regressors to variables from GAEZ. This excludes variables capturing geographical features such as distance to the coast or ruggedness that do not change between 2010 and 2100.

In this case, as the figure shows, the projected impact of climate change is almost uniformly less negative (or more positive) using the restricted specification than in our baseline. Further, the projected impact of climate change on world GDP is positive in the restricted specification vs. negative in our baseline, and even focusing on countries with below median income, the projected negative impact is 50% larger in absolute value in the baseline specification than in the restricted version.

Figure F2: GAEZ Variables Only

(a) Log Difference of Location Quality

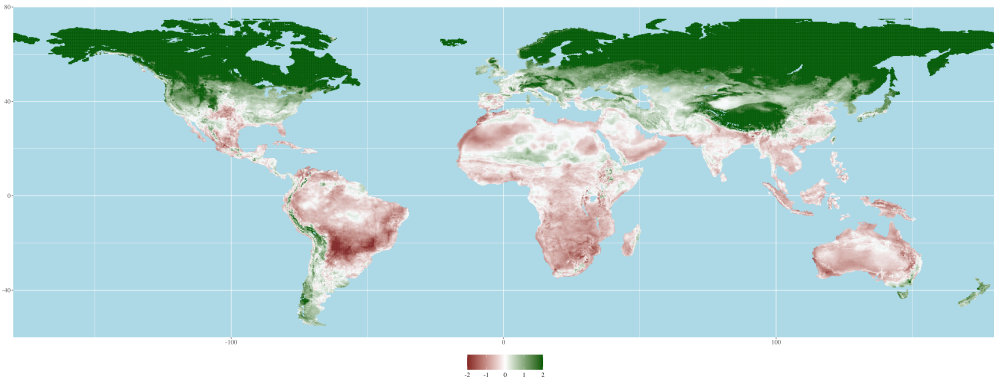

(b) Country-Level Log Difference in *ALQ*

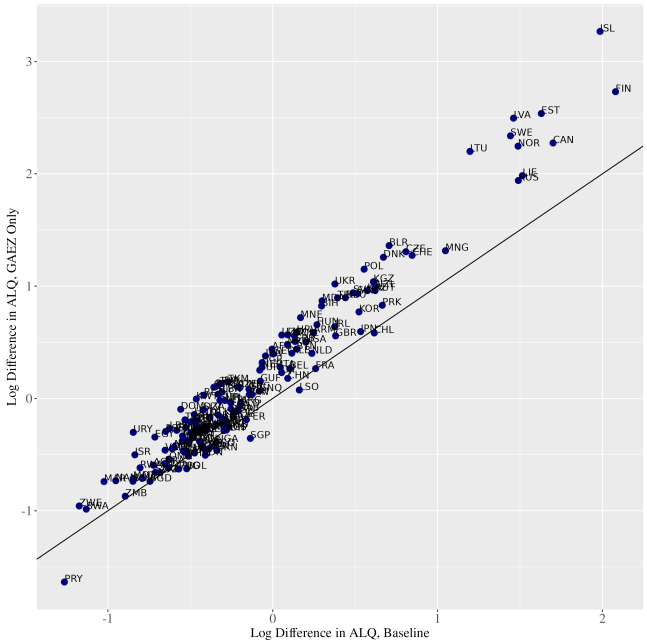

Table F2: 2100 Impacts as Percentage of Aggregate GDP

Sample	Full			Below Median Income		
	SSP	RFF-SP Impact		SSP	RFF-SP Impact	
Scenario	Impact	Mean	SD	Impact	Mean	SD
RCP 2.6	2.06	3.63	1.00	−0.77	−0.65	0.37
RCP 4.5	4.02	5.87	1.44	−0.17	−0.26	0.48
RCP 6.0	5.32	5.58	1.71	−1.91	−2.09	0.76
RCP 8.5	4.05	6.01	2.61	−6.24	−5.06	1.60

Note: Results aggregate 156 countries in the full sample and 78 countries in the below median income countries sample. Impacts are in percentages.

F.3 Trade interactions

The baseline specification comprises both time-invariant geographic features and characteristics affected by climate change. The former includes variables that reflect suitability for trade, which may interact with agroclimatic variables in determining land quality. We explore this possibility by generating land quality with a Poisson regression in which each variable that changes with climate change is interacted with five geographic variables relevant to trade from the baseline regression: distance to the

coast, ruggedness, and the existence of coasts, navigable rivers, and natural harbors within 25 km of the cell centroid.[7] Appendix Figure F3a maps the change in location quality from 2010 to 2100 under RCP 8.5, while F3b aggregates these changes at the country level and plots them against the country-level changes in the baseline specification.

Figure F3: GAEZ interacted with trade variables

(a) Log Difference in Location Quality

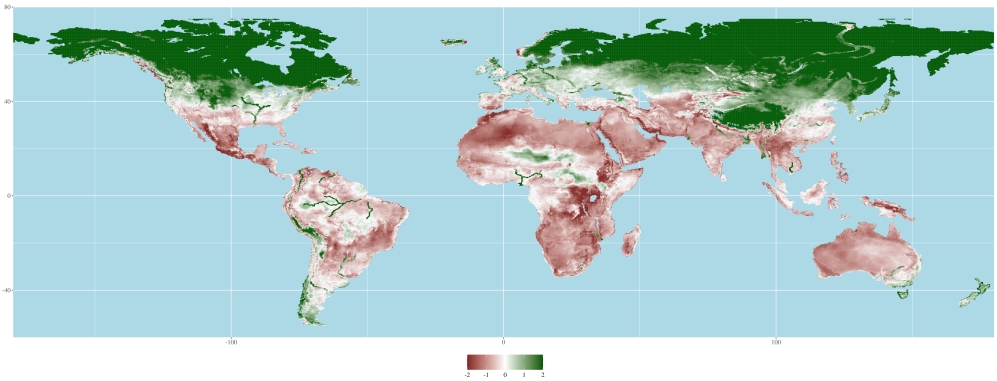

(b) Country-Level Log Difference in *ALQ*

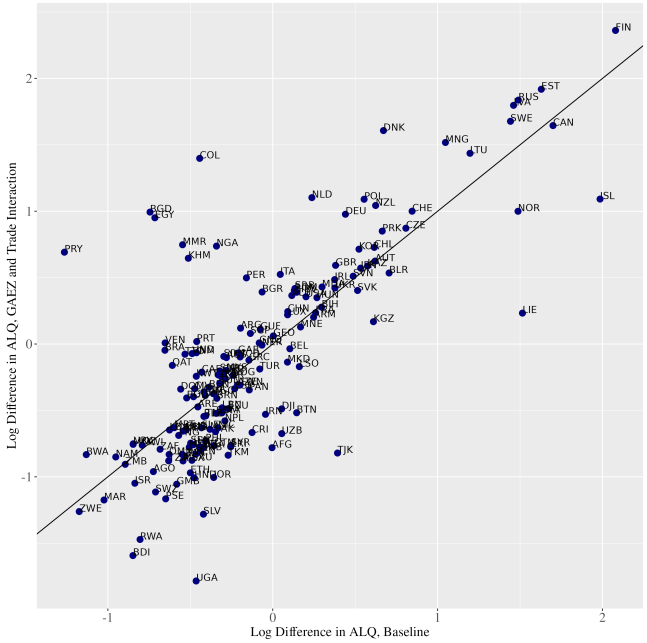

[7]The indicator denoting proximity to lake was omitted, and nontrade geographic variables were included only as controls.

On the grid-cell level, the most notable change is that this interacted specification projects large climate-induced improvements in land quality near rivers.[8] Aggregating to countries, the match between the baseline and interacted specifications is not as tight as in the two previous alternative specifications that we considered. Specifically, the interacted specification projects much better outcomes for several countries that contain rivers (Paraguay, Egypt, Myanmar, Nigeria), and significantly worse outcomes for several landlocked ones (Uganda, Burundi, Rwanda). Overall, the interacted specification predicts a rise in world GDP in response to climate change, and even among countries with below-median GDP, the projected negative effect is less than half as large as in the baseline specification.

Table F3: 2100 Impacts as Percentage of Aggregate GDP

Sample	Full			Below Median Income		
	SSP	RFF-SP Impact		SSP	RFF-SP Impact	
Scenario	Impact	Mean	SD	Impact	Mean	SD
RCP 2.6	−0.26	1.75	1.04	−2.91	−1.41	1.17
RCP 4.5	1.45	3.56	1.56	−2.01	−0.74	1.81
RCP 6.0	3.55	3.88	1.75	−1.48	−1.21	2.03
RCP 8.5	4.45	5.66	2.27	−2.41	−0.55	2.37

Note: Results aggregate 156 countries in the full sample and 78 countries in the below median income countries sample. Impacts are in percentages.

G Derivations of the Change in the K/Y Ratio

G.1 Perfect Mobility

In the perfect mobility case, the last term of equation (13) is derived as follows. We assume that capital is accumulated in the usual Solow model fashion

$$\dot{K} = sY - \delta K, \tag{G2}$$

where δ is the rate of depreciation and the saving rate s is assumed to be fixed. Romer (2012) shows that if the rates of saving, depreciation, population growth, and

[8] One issue with including all interactions of trade and agroclimatic variables is that the number of regressors balloons to 283, raising concerns of overfitting. To address this, we fit Poisson models with the Least Absolute Shrinkage and Selection Operator (Lasso) estimator on the full set of interactions for a more parsimonious model but did not find notable improvement. Results are available upon request.

technological progress are constant, then along the balanced growth path the capital-output ratio, which is the second term in equation (12), converges to a constant. Taking logs of (12), differentiating with respect to time, and then rearranging, we can solve for the growth rate of total output:

$$\hat{Y} = \frac{\phi\hat{X} + (1-\alpha-\phi)[\hat{e}+\hat{L}]}{1-\alpha} \tag{G3}$$

We can similarly write the equation for the growth rate of capital as

$$\hat{K} = s\Big(\frac{Y}{K}\Big) - \delta. \tag{G4}$$

Equating (G4) to (G3), the capital-output ratio along the balanced growth path is

$$\frac{K}{Y} = \frac{s}{\delta + \frac{\phi\hat{X}+(1-\alpha-\phi)[\hat{e}+\hat{L}]}{1-\alpha}}. \tag{G5}$$

Thus

$$\left(\frac{(K/Y)_{alt}}{(K/Y)_{base}}\right) = \frac{\delta(1-\alpha)+(1-\alpha-\phi)[\hat{e}+\hat{L}_{base}]+\phi\hat{X}_{base}}{\delta(1-\alpha)+(1-\alpha-\phi)[\hat{e}+\hat{L}_{alt}]+\phi\hat{X}_{alt}} \tag{G6}$$

Further assuming that the growth of population and location quality are both constant on the balanced growth path, $\hat{L}$ and $\hat{X}$ are the annualized growth rates between 2010 and 2100 of population and aggregate location quality in either the baseline or alternative scenario. That is,

$$\hat{L} = \frac{ln(L_{2100}) - ln(L_{2010})}{90} \tag{G7}$$

and

$$\hat{X}_{alt} = \frac{ln(X_{alt,2100}) - ln(X_{alt,2010})}{90} \tag{G8}$$

where, omitting the normalization constant, $X_i = Z_i exp(x_i\hat{\beta})$. In the baseline case, location quality does not change between 2010 and 2100; it follows that $\hat{X}_{base} = 0$.

G.2 Perfect Mobility with Unmeasured Quality

As in the case of Perfect Mobility, we continue to assume that output per worker is equalized across grid squares in a country in both the present and future. The derivation of the last term in equation (18) is thus identical to equation (G6). How-

ever, we now include unmeasured quality in our location quality measure, and thus $X_i = Z_i exp(x_i\hat{\beta})\epsilon_i$. We make use of equation (17) and the fact that $X_{alt,2010} = X_{base,2010} = X_{base,2100}$ to derive the new $\hat{X}_{alt}$:

$$\hat{X}_{alt} = \frac{ln(\frac{X_{alt,2100}}{X_{alt,2010}})}{90} = \frac{ln\left(\sum_i \left(\frac{L_{i,base}}{L_{base}}\right) \frac{exp(x_{i,alt}\hat{\beta})}{exp(x_{i,base}\hat{\beta})}\right)}{90} \tag{G9}$$

$\hat{L}$ and $\hat{X}_{base}$ remains the same as the previous case.

G.3 No Mobility Going Forward

With no mobility going forward, output per worker is no longer equalized across grid cells in the future. Instead of using (12) as in the cases of Perfect Mobility and Perfect Mobility with Unmeasured Quality, we sum (10) across grid cells to solve for total output:

$$Y = \sum_i Y_i = \left(\frac{K}{Y}\right)^{\alpha/(1-\alpha)} e^{(1-\alpha-\phi)/(1-\phi)} \sum_i \left(L_i^{(1-\alpha-\phi)/(1-\alpha)} X_i^{\phi/(1-\alpha)}\right) \tag{G10}$$

Taking logs of (G10), differentiating with respect to time, and rearranging yields the growth rate of total output:

$$\hat{Y} = \frac{1-\alpha-\phi}{1-\alpha}\hat{e} + \frac{\sum_i \left(L_i^{(1-\alpha-\phi)/(1-\alpha)} X_i^{\phi/(1-\alpha)} \left(\frac{1-\alpha-\phi}{1-\alpha}\hat{L}_i + \frac{\phi}{1-\alpha}\hat{X}_i\right)\right)}{\sum_i \left(L_i^{(1-\alpha-\phi)/(1-\alpha)} X_i^{\phi/(1-\alpha)}\right)} \tag{G11}$$

As before, the growth rate of capital is (G4).

Equating (G4) to (G11), the capital-output ratio along the balanced growth path is

$$\frac{K}{Y} = \frac{s}{\delta + \frac{1-\alpha-\phi}{1-\alpha}\hat{e} + \frac{\sum_i \left(L_i^{(1-\alpha-\phi)/(1-\alpha)} X_i^{\phi/(1-\alpha)} \left(\frac{1-\alpha-\phi}{1-\alpha}\hat{L}_i + \frac{\phi}{1-\alpha}\hat{X}_i\right)\right)}{\sum_i \left(L_i^{(1-\alpha-\phi)/(1-\alpha)} X_i^{\phi/(1-\alpha)}\right)}} \tag{G12}$$

Thus

$$\left(\frac{(K/Y)_{alt}}{(K/Y)_{base}}\right) = \frac{\delta(1-\alpha) + (1-\alpha-\phi)\left[\hat{e} + TL_{base}\right] + \phi T X_{base}}{\delta(1-\alpha) + (1-\alpha-\phi)\left[\hat{e} + TL_{alt}\right] + \phi T X_{alt}} \tag{G13}$$

with

$$TL_{base} \equiv \sum_i \frac{L_{i,base}^{\frac{1-\alpha-\phi}{1-\alpha}} X_{i,base}^{\frac{\phi}{1-\alpha}}}{\sum_i L_{i,base}^{\frac{1-\alpha-\phi}{1-\alpha}} X_{i,base}^{\frac{\phi}{1-\alpha}}} \hat{L}_{i,base}, \; TX_{base} \equiv \sum_i \frac{L_{i,base}^{\frac{1-\alpha-\phi}{1-\alpha}} X_{i,base}^{\frac{\phi}{1-\alpha}}}{\sum_i L_{i,base}^{\frac{1-\alpha-\phi}{1-\alpha}} X_{i,base}^{\frac{\phi}{1-\alpha}}} \hat{X}_{i,base}$$

and TL_{alt} and TX_{alt} defined analogously.

(G13) is analogous to (G6) except $\hat{L}$ and $\hat{X}$ are replaced by TL and TX respectively. TL and TX are the output weighted averages of the growth rate of grid cell i's population and of the growth rate of grid cell i's location quality.

G.4 Quantitative Importance of the K/Y Term

Appendix Table G1, for the case of perfect mobility, shows that the term representing the change in the K/Y ratio contributes extremely little to variation across countries in projected climate impacts, and is very insensitive to the choice of $\hat{e}$.

Table G1: Variance Decomposition of Impact Estimates

	Variance				$2 \times$ Covariance		
$\hat{e}$	$\frac{Y}{L}$	X	L	$\frac{K}{Y}$	X, L	X, $\frac{K}{Y}$	L, $\frac{K}{Y}$
0 %	0.155	0.042	0.059	0.001	0.040	-0.000	0.014
1 %	0.154	0.042	0.059	0.001	0.040	-0.000	0.012
2 %	0.152	0.042	0.059	0.001	0.040	-0.000	0.011

Note: This table shows decompositions of the logarithmic version of equation (13), for different values of the productivity growth parameter $\hat{e}$.

References

Carneiro Freire, SM, K Macmanus, M Pesaresi, E Doxsey-Whitfield, and J Mills (2016) "Development of new open and free multi-temporal global population grids at 250 m resolution," in Tapani Sarjakoski, Maribel Yasmina Santos and L. Tiina Sarjakoski eds. *Proceedings 2016: The 19th AGILE International Conference on Geographic Information Science*: AGILE.

Chan, Duo, Alison Cobb, Lucas R Vargas Zeppetello, David S Battisti, and Peter Huybers (2020) "Summertime temperature variability increases with local warming in midlatitude regions," *Geophysical Research Letters*, 47 (13), e2020GL087624.

Corbane, Christina, Aneta Florczyk, Martino Pesaresi, Panagiotis Politis, and Vasileios Syrris (2018) "GHS built-up grid, derived from Landsat, multitemporal

(1975-1990-2000- 2014), R2018A," published data package, European Commission, Joint Research Centre (JRC).

Corbane, Christina, Martino Pesaresi, Thomas Kemper et al. (2019) "Automated global delineation of human settlements from 40 years of Landsat satellite data archives," *Big Earth Data*, 3 (2), 140–169.

Florczyk, A, C Corbane, D Ehrlich et al. (2019) "GHSL Data Package 2019,"Technical report, Joint Research Center, Luxembourg (Luxembourg).

Frankcombe, LM, MH England, JB Kajtar, ME Mann, and BA Steinman (2018) "On the choice of ensemble mean for estimating the forced signal in the presence of internal variability," *Journal of Climate*, 31 (14), 5681–5693.

Galor, Oded and Ömer Özak (2016) "The agricultural origins of time preference," *American Economic Review*, 106 (10), 3064–3103.

Henderson, J Vernon, Tim Squires, Adam Storeygard, and David Weil (2018) "The global distribution of economic activity: nature, history, and the role of trade," *Quarterly Journal of Economics*, 133 (1), 357–406.

Romer, David (2012) *Advanced Macroeconomics*, New York: McGraw-Hill Irwin.

Rose, Amy N. and Eddie A. Bright (2014) "The LandScan Global Population Distribution Project: Current State of the Art and Prospective Innovation," Paper presented at Population Association of America Annual Meeting.

Schiavina, Marcello, Sergio Freire, and Kytt MacManus (2019) "GHS population grid multi-temporal (1975-1990-2000-2015), R2019A,"Technical report, European Commission, Joint Research Centre (JRC).